

March 1989

Los Alamos National Laboratory is operated by the University of California for the United States Department of Energy under contract W-7405-ENG-36

LA-UR--89-479

DE89 007980

TITLE ALEXIS: A narrow-Band Survey/Monitor of the Ultrasoft X-Ray Sky

AUTHOR(S) W. C. Friedhorsky, J. J. Bloch, F. Cordova, B. W. Smith,
M. Ulibarri, Los Alamos National Laboratory
J. Chavez and E. Evans, Sandia National Laboratory
O. H. W. Siegmund, H. Marshall, J. Vallerga, P. Vedder,
Space Sciences Laboratory/UC Berkeley

SUBMITTED TO Proceedings from The Berkeley Colloquium on Extreme Ultraviolet
Astronomy

DISCLAIMER

This report was prepared as an account of work sponsored by an agency of the United States Government. Neither the United States Government nor any agency thereof nor any of their employees makes any warranty, express or implied, or assumes any legal liability or responsibility for the accuracy, completeness, or usefulness of any information, apparatus, or method or process disclosed, or represents that it would not infringe privately owned rights. References to specific commercial products, processes, or services by trade names, trademarks, or otherwise, does not necessarily constitute or imply endorsement, recommendation, or approval by the United States Government or any agency thereof. The views and opinions of authors expressed herein do not necessarily state or reflect those of the United States Government or any agency thereof.

By acceptance of this article, the publisher recognizes that the U.S. Government retains a nonexclusive, royalty-free license to publish or reproduce the published form of this contribution or to allow others to do so for U.S. Government purposes.

The Los Alamos National Laboratory requests that the publisher identify this article as work performed under the auspices of the U.S. Department of Energy.

Los Alamos Los Alamos National Laboratory
Los Alamos, New Mexico 87545

ALEXIS: A Narrow-Band Survey/Monitor of the Ultrasoft X-Ray Sky

W. C. Friedhorsky, J. J. Bloch, F. Córdova, B. W. Smith, and M. Ulibarri
Los Alamos National Laboratory

J. Chavez and E. Evans
Sandia National Laboratory

O. H. W. Siegmund, H. Marshall, J. Vallerger, and P. Vedder
Space Sciences Laboratory/UC Berkeley

Abstract

Los Alamos and Sandia National Laboratories are building an ultrasoft X-ray monitor experiment. This experiment, called ALEXIS (Array of Low-Energy X-Ray Imaging Sensors), consists of six compact normal-incidence telescopes. ALEXIS will operate in the range 70 - 110 eV.

The ultrasoft X-ray/EUV band is nearly uncharted territory for astrophysics. ALEXIS, with its wide fields-of-view and well-defined wavelength bands, will complement the upcoming NASA Extreme Ultraviolet Explorer and ROSAT EUV Wide Field Camera, which are sensitive broad-band survey experiments. The program objectives of ALEXIS are to 1) demonstrate the feasibility of a wide field-of-view, normal incidence ultrasoft X-ray telescope system and 2) to determine ultrasoft X-ray backgrounds in the space environment. As a dividend, ALEXIS will pursue the following scientific objectives: 1) to map the diffuse background, with unprecedented angular resolution, in several emission-line bands, 2) to perform a narrow-band survey of point sources, 3) to search for transient phenomena in the ultrasoft X-ray band, and 4) to provide synoptic monitoring of variable ultrasoft X-ray sources such as cataclysmic variables and flare stars.

The six ALEXIS telescopes are arranged in pairs to cover three 33° fields-of-view. During each spin of the satellite, ALEXIS will monitor more than half the sky. Each telescope consists of a layered synthetic microstructure (LSM) mirror, a curved microchannel plate detector, background-rejecting filters and magnets, and readout electronics. The mirrors will be tuned to 72 eV, 85 eV, and 95 or 107 eV bands, chosen to select and deselect interesting line features in the diffuse background.

The geometric area of each ALEXIS telescope will be about 25 cm^2 . The telescopes employ spherical mirrors with the curved detector at prime focus and are limited by spherical aberration to a resolution of about $0.5''$. Assuming nominal reflectivities, quantum efficiency, and filter transmission, the 5σ survey sensitivity will be several $\times 10^{-3} \text{ photons cm}^{-2} \text{ s}^{-1}$ for line emission at the center of the bandpass.

ALEXIS is designed to be flown on a small autonomous payload carrier (a minisat) that could be launched from any expendable launch vehicle. The experiment weighs 700 pounds, draws 40 watts, and produces 10 kbps of data. It can be flown in any low Earth orbit. Onboard data storage allows operation and tracking from a single ground station at Los Alamos.

1. INTRODUCTION

The region between the ultraviolet and soft X-ray bands is one of the last to be surveyed by astronomers. Though interstellar absorption limits visibility to relatively nearby objects, the extreme ultraviolet/ultrasoft X-ray band ($\sim 15\text{-}125$ eV) should provide a unique probe of the hot interstellar medium, hot degenerate stars, mass transfer binaries, flare stars, and other nearby, energetic systems. This region of the spectrum is ripe for discovery, as Martin Harwit points out in *Cosmic Discovery* (Harwit 1981), astronomical discovery comes from expanding the observational phase space of wavelength, polarization, and spectral, spatial, and time resolution. One window into this band will open with the Wide Field Camera on the British German-US ROSAT mission, scheduled for launch in 1990 (Trumper 1984) and NASA's Extreme Ultraviolet Explorer, scheduled for launch in 1991 (Malina *et al.* 1987). These telescopes will survey the sky with high angular resolution, high sensitivity, a few degrees field of view, and broad spectral response and thereby study persistent point sources in this band. An complementary window into the ultrasoft X-ray domain can be provided by a wide field-of-view, narrow band instrument sensitive to transient phenomena and structure in the ultrasoft X-ray background. We propose to open this window with an experiment called ALEXIS.

ALEXIS (Array of Low-Energy X-Ray Imaging Sensors) is an array of normal-incidence ultrasoft X-ray telescopes designed for flight on a miniature satellite (minisat). The project is led by Los Alamos National Laboratory, with collaborators at Sandia National Laboratory and the Space Sciences Laboratory/University of California at Berkeley. The mission objectives of ALEXIS are 1) to demonstrate the feasibility of a wide field-of-view, normal-incidence telescope system for detecting bursts of ultrasoft X-rays and 2) to determine the background rate of ultrasoft X-ray bursts and events that mimic them, in the space environment. In doing so, we will build the first ultrasoft X-ray instrument with a very wide field-of-view and a well-defined spectral response, and thus 1) map the diffuse background, with unprecedented angular resolution, in several emission line bands, 2) perform a narrow-band survey of point sources, 3) provide synoptic monitoring of variable ultrasoft X-ray sources such as cataclysmic variables and flare stars, and 4) search for transient phenomena in the ultrasoft X-ray band. The ALEXIS experiment was described by Friedhorsky *et al.* (1988); this paper is a more comprehensive treatment, and represents further development of the experiment.

The ALEXIS telescopes are made possible by the maturation of two technologies. First, layered synthetic multistructures are now commercially available, allowing normal incidence optics in the ultrasoft X-ray band (e.g., Barbee 1985); second, microchannel plate technology has matured to allow production of steeply curved, high position resolution, low-background ultrasoft X-ray detectors. With these components, we will build the simplest possible telescope system: a spherical mirror with detector at the prime focus. The modest angular resolution is more than offset by advantages of wide field-of-view, high efficiency, and simplicity of fabrication and alignment.

To minimize mission cost and maximize the possibilities for launch, we have designed ALEXIS around a minisatellite bus that can be launched from any expendable launch vehicle and that can fly in any low earth orbit. We can thus fly a significant space experiment for a few million dollars. The minisatellite spins about an axis pointed at the Sun. During each spacecraft spin, the telescope array sweeps out more than half the sky. ALEXIS thus monitors each ultrasoft X-ray source for at least 6 months per year.

This paper summarizes the technological approach and scientific promise of the ALEXIS experiment. In Section 2, we consider the optical design, both the imaging characteristics and the expected layered synthetic multistructure performance. In Section 3, we discuss our curved surface microchannel plate detectors. Section 4 considers background sources and how they can be overcome. In section 5 we discuss the high dynamic range electronics needed to detect both ultrasoft X-rays and bursts of ultrasoft X-rays. Section 6 discusses the on-board hardware and software needed to calculate telescope event positions and the downstream handling of these data. Section 7 discusses the overall experiment envelope and the interface with the minisat. In Section 8, we discuss the ground support hardware and software. Section 9 concludes this paper with a discussion of ALEXIS's scientific objectives and sensitivity.

2. OPTICAL DESIGN

2.1 Imaging Performance

The development of layered synthetic microstructures (LSMs) allows the use of normal incidence optics in the ultrasoft X-ray region. ALEXIS takes advantage of this possibility by using compact, simple, single reflection telescopes. However, the single-reflection telescope is limited to fields of view of about 40° (full width) and has considerable spherical aberration. Nonetheless, it offers simplicity of assembly and fabrication as well as high throughput, enough to justify its choice as the first LSM optics for orbital application.

Figure 1 shows the simplest possible reflection telescope: a spherical mirror with a detector at prime focus. This design is well suited for LSM optics, because of the single-reflection light path (peak reflectivities of multilayers are not high, so multiple reflections are costly in efficiency) and because the spherical surface is easy to fabricate with the high-quality surface finish required for good reflectivity.

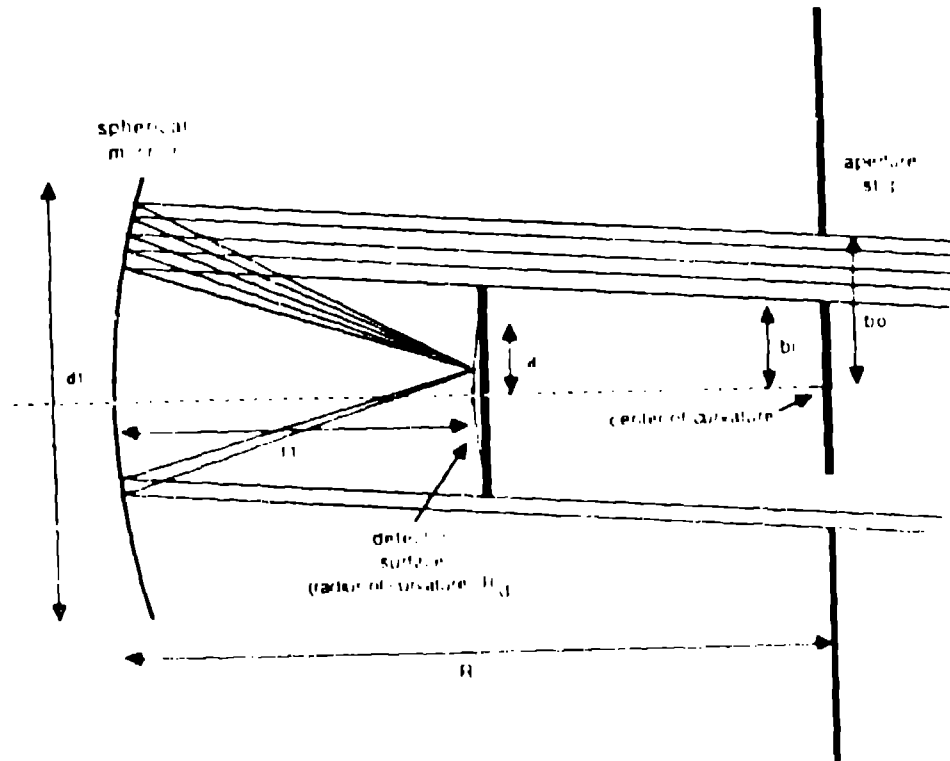


Figure 1. Optical design of the spherical prime focus telescope used in ALEXIS.

This system is limited in field of view and spatial resolution. Field of view is limited because the detector can be no larger than the aperture, or it will block the incoming radiation. In the paraxial approximation ($\theta \ll 1$, where θ is the focal ratio) the field of view $\Delta\theta$ (full width) is thus

$$\Delta\theta = 2 \sin^{-1}(a/l_1) = 2 \sin^{-1}(f^{-1}hg/2) \approx f^{-1}hg \text{ radians,}$$

$f = l_1/2b_0$, h is the fraction of the aperture filled by the detector body, b_1/b_0 , and g is the fraction of the detector aperture which is active, a/b_1 . By pushing each of these parameters as far as possible, i.e., $f = h = g = 0.5$, one could obtain a field of view of about 40° (full width). The mirror has a very low f number, which leads to large spherical aberration. The resolution (full width) of a fully illuminated spherical optic is

$$\Delta\Phi = 1/128 f^3 \text{ radians,}$$

or, for example, 7.8 milliradians for an $f/1$ optic. Here, Φ corresponds to position along the focal plane in units of incident angle.

We improve the resolution of a spherical reflection telescope by placing an annular aperture stop before the mirror. This limits the impact parameters of the rays incident upon the mirror as the annulus approaches zero width, the blur goes to zero. When placed at the center of curvature of the spherical mirror, the aperture appears the same (except for elliptical foreshortening) for rays on- and off-axis. We thus ensure nearly uniform resolution over the field-of-view.

The ALEXIS dimensions finally chosen are $R=13.52$ cm, $b_i=2.80$ cm, $b_o=3.925$ cm, and $R_d=7.0$ cm. The focal distance, f_f , is thus 6.52 cm. The primary thus has an unfilled aperture of speed $f/0.83$. Because the detector surface is concentric with the mirror, the resolution is nearly constant over the 33° (diameter) field-of-view. The spot size is 0.20° (rms radius). Figure 2 shows the telescope geometric area and rms resolution as a function of off-axis angle, as calculated by a Monte Carlo ray trace code. The area-solid angle product of the telescope is 4.3 cm² steradians. Obscuration by the detector introduces a significant asymmetry in the image at large off-axis angles.

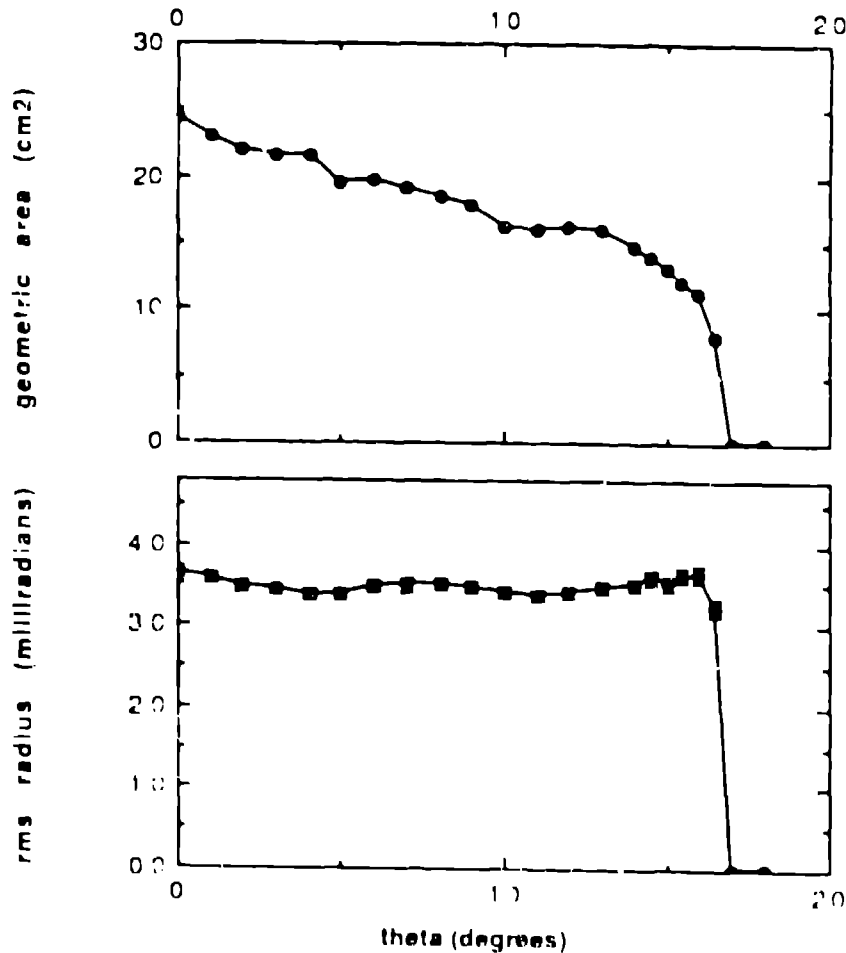


Figure 2. Geometric area and resolution (radius rms) for the ALEXIS telescope, as a function of off-axis angle.

2.2 Layered Synthetic Microstructure (LSM) Performance

ALEXIS depends on layered synthetic microstructure (LSM) mirrors, or "multilayers", for normal incidence reflection in the 72, 85, and 105 eV bands. To work well, these mirrors must have high reflectivity in the selected band and low reflectivity for He II $\lambda 304 \text{ \AA}$ (41 eV) and Ly $\alpha \lambda 1216 \text{ \AA}$ backgrounds. The ALEXIS LSMs will convert

of alternating layers of a material which is reflective in the EUV, molybdenum, and a spacer, either silicon or boron carbide. Experimental reflectivities greater than 0.5 at normal incidence have been reported for Mo-Si LSMs in the EUV (73-78 eV, Barbee, Mrowka, and Heitnick 1985). We have made our own theoretical calculations of multilayer mirror reflectivities, which have been recently verified by measurements of a test mirror.

Our test mirror, which was obtained from Ovonic, Inc., had the following characteristics: spacing of Mo layers, $d = 100 \text{ \AA}$, thickness of Mo layers, $\gamma d = 33 \text{ \AA}$, thickness of Si layers, $(1-\gamma)d = 67 \text{ \AA}$ (all values $\pm 2 \text{ \AA}$), 50 pairs of Mo/Si layers with Mo on top, a quartz substrate, and at least 10 \AA of carbon as the first surface. The reflectivity of this mirror was measured at 13.1° off normal incidence, somewhat less than the best effective angle for peak reflectivity, which is calculated to be 23° off normal. The results were (R = reflectivity)

Wavelength	R _{measured}	R _{calculated}
171 \AA	.022	.022
256 \AA	.022	.012
304 \AA	.036	.011
584 \AA	.052	.068
1216 \AA	.036	.104

The calculations used the optical constants for Mo and Si measured by Windt (1987), which were measured from samples somewhat contaminated with oxygen. The agreement is not perfect, but several features emerge. The calculations show that carbon damages the performance of the mirror both at the peak (computed to be $R(171 \text{ \AA}) = .17$) and at 304 \AA . Without the carbon first surface, the peak is predicted to be $R(171 \text{ \AA}) = .44$ and $R(304 \text{ \AA})$ is reduced by more than a factor of 2. However, the reflectivity at 1216 \AA increases drastically without the carbon. Oxygen contamination, which can be present in silicon films, also decreases reflectivity at most wavelengths.

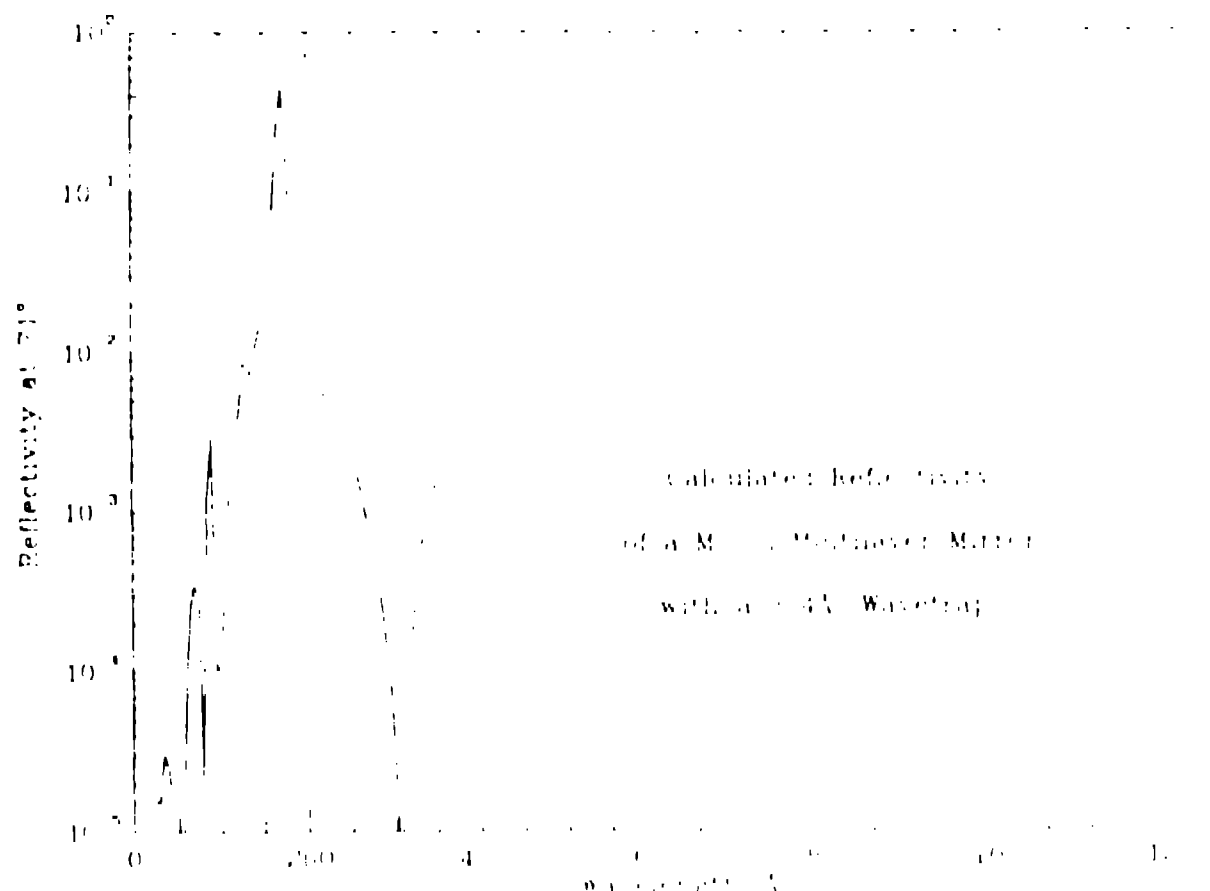


Figure 3. Calculated reflectivity of the 304 \AA reflecting LSM described above.

In order to obtain reflectivity at the working wavelength good enough to produce the desired sensitivity, we need to maintain a high peak reflectivity at 171 Å while minimizing the reflectivity at background wavelengths (286 Å, 304 Å, 584 Å, and 1216 Å). The first requirement, a high peak reflectivity, forces elimination of all oxygen and carbon from the multilayer, leaving us with a problem at long background wavelengths that must be corrected in the filters. The most damaging background line is He II λ 304 Å, because it cannot be filtered out without also filtering the working wavelength. We have devised a "wavetrapp" to eliminate 304 Å background by adding two layer pairs on top of the Mo/Si multilayer. These layers are almost transparent at 171 Å but interfere destructively at 304 Å. The design consists of (beginning from the first surface) two layer pairs, each 10 Å Mo and 55 Å Si, over 40 layer pairs, each 30 Å Mo and 64 Å Si. The calculated reflectivities of this mirror are $R(171 \text{ Å}) = .44$, $R(286 \text{ Å}) = .018$, $R(304 \text{ Å}) = .000004$, $R(584 \text{ Å}) = .089$, and $R(1216 \text{ Å}) = .48$, at 19 degrees off normal incidence, which is the average reflection angle for the ALEXIS telescopes. We used the optical constants for Si from Palik (1985). The high reflectance at 584 Å and 1216 Å can be filtered out. A wavetrapp is not feasible at 584 Å, because there is little contrast in index of refraction for most materials. Mirrors for other wavelength bands will be designed similarly.

3. MICROCHANNEL PLATE DETECTORS

By symmetry, the spherical telescopes described above have a spherical focal surface; the radius of this surface is approximately half the radius of the spherical mirror. The detector must determine the position of ultrasoft X-rays and bursts of ultrasoft X-rays that arrive at this surface, with a position resolution commensurate with (2 to 3 times oversampling) the telescope point-spread function. We plan to develop and fabricate curved-surface microchannel plate (MCP) detectors by straightforward modification of a standard planar detector scheme (Siegmund *et al.* 1987). The MCP stack will consist of a pair of plates with 120:1 channel-length-to-diameter (12.5 μm channels) ratio. Each MCP will be curved in such a fashion to allow back-to-back stacking of the MCPs, with the front surface having the desired radius of curvature. An incident photon will interact with an opaque photocathode layer, probably MgI₂, deposited on the front MCP. This interaction results in a photoelectron that is multiplied by the MCP stack to yield more than 1×10^7 electrons at the MCP output. The electron cloud drifts over a 15 mm gap and is collected by a wedge-and-strip anode, where the incident charge is divided between three electrodes (Siegmund *et al.* 1986). The areas of the wedge and strip electrodes vary linearly in area with the X and Y coordinates, respectively. Therefore the charge signal observed on the wedge and strip, normalized by division by the total incident charge, gives the position of the charge cloud and hence the location of the incident photon.

ALEXIS Curved Microchannel Plate Detector Schematic

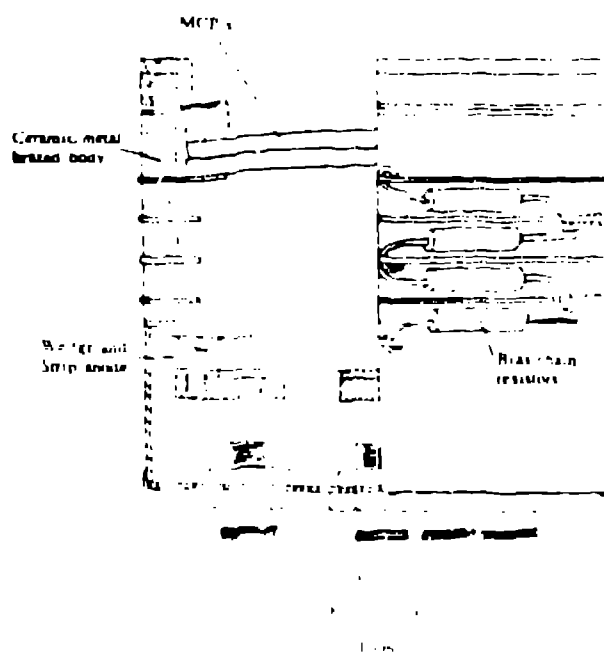


Figure 4. Schematic of the curved MCP detector for ALEXIS.

The detector front is curved with a radius of 7.0 cm to correspond to the focal plane of the spherical mirror. The outer diameter is critical; in a prime focus design, the detector must not obscure the mirror. The outer diameter must thus be minimized for a given effective aperture. Figure 4 shows a schematic of the detector designed to use two curved MCPs. The active diameter will be 40 mm and the outer diameter of the MCPs is 46 mm. The detector body, fabricated using alumina ceramic and kovar brazed at high temperature, has an outer diameter less than 56 mm and a length less than 50 mm, meeting our requirement of minimum obscuration. This type of construction is used in ultra-high-vacuum image-tube devices, and will be compatible with vacuum and cleanliness requirements for an ultrasoft X-ray detector. Devices of a similar design have been built for the FAUST (Deharveng *et al.* 1979) program, and these have withstood several vibration tests and a rocket payload launch.

For adequate input to the front-end electronics, a MCP gain in excess of 1×10^7 will be required, with a relatively narrow pulse height distribution. Background rates must be below $1 \text{ event cm}^{-2} \text{ sec}^{-1}$ so as not to overload the telemetry, and to allow good signal-to-noise in measurements of the diffuse background. In the UCB SSF program, we normally use a stack of 3:80:1 length/diameter ratio (L/D) back-to-back MCPs to achieve the characteristics. However, since this scheme would result in two interfaces between curved surfaces, it increases the possibility of gain variations due to possible interplate gaps. We have therefore chosen a pair of back-to-back MCPs each with a 120:1 L/D ratio. This scheme (Fraser *et al.* 1983) has worked for flat MCP stacks and gives gain and pulse height distribution performance close to that of the three MCP configuration. We have also evaluated MCP stacks with this configuration having a 50 cm radius of curvature and found them to be satisfactory (Siegmund 1988). The MCP channels will be perpendicular to the surface of the front plate and biased at 13° in the second. To meet the background requirement, residual radioactivity in the MCP glass must be minimal; the MCP glass must be rubidium-free but may contain potassium (Siegmund *et al.* 1988).

Boules of the required standard MCP material will be procured, and thick slices taken from them. These slices will then be ground to the correct radius of curvature, polished, etched to open the MCP channels, and the final processing steps performed. The exact surface curvatures are such that the centers of the MCPs will touch when stacked. Then, when the MCPs are clamped into place, the edges of the plates will also come into contact. We have previously employed this technique, and shown that it is effective in avoiding gaps between the MCPs that would cause gain variations (Siegmund 1988).

The wedge-and-strip anode will use a standard design scheme (Siegmund *et al.* 1986). This employs a three-electrode pattern—50 mm in diameter with a repulsion period of ~ 1 mm. The fractional area covered by the wedge-and-strip anodes varies from about 0.067 to 0.333 across the field of view. This pattern type has already been used in several detectors and has achieved better than 60 μm FWHM resolution (Siegmund *et al.* 1987). The anode will be etched into a thin copper layer ($\sim 6 \mu\text{m}$) applied to a curved fused quartz substrate, which can be purchased economically as a suck lens. In the drift gap between MCP and anode, the electron image will be reduced from the scale at the microchannel plate, allowing a smaller anode which fits the overall diameter constraint. Since a curved surface cannot map without distortion onto a plane, we expect some image distortion. This should be stable and can be accommodated by mapping the detector. We do not expect this configuration to significantly degrade the resolution of the detector compared to flat MCP devices. For standard single-event electronics (preamplifier noise 1600 e⁻ rms for the wedge and strip anodes, and 1900 e⁻ rms for the zig zag), the position resolution should be about 50 μm FWHM. As discussed below, the resolution will be necessarily less for the high-dynamic range electronics used in ALEXIS. Magnetic fields in the 15 mm drift gap can distort the image and must be limited to $\sim 1/2$ Gauss; this is achieved by magnetic shielding placed outside the back of the detector.

A photocathode layer, probably MgF_2 , will be deposited on the top of the first MCP. Approximately 10,000 Å of MgF_2 will be evaporated onto the MCP surface at a rate less than 50 Å sec^{-1} , while the MCP is heated to $\sim 10^\circ \text{C}$ and rotated about the MCP channel axis. The evaporation angle to the microchannel axis will be about 15° , giving a cathode layer thickness of about 1000 Å inside the channels. The Berkeley group has made a number of MgF_2 photocathodes in this fashion; typically, the quantum efficiency is $\sim 30\%$ in the range 100–200 Å. The cathodes are generally very stable, but we will still attempt to minimize exposure to the atmosphere after deposition.

Thin film filters will be placed in front of the microchannel plate detectors. These perform two main functions: 1) to exclude unwanted radiation at wavelengths outside the bandpass, and 2) to block low-energy charged particle impact. Candidate filter materials are Lexan/Boron and Aluminum/Carbon. These filters provide broad bandpasses centered at 120 eV and 60 eV, respectively (Vallerga *et al.* 1986). Lexan/Boron would be used for the short bandpass telescopes (85 eV and 10³ eV) and Aluminum/Carbon for the long wavelength telescopes (2 eV). These filters will be optimized to reduce the geocoronal background flux (He II $\lambda 304 \text{ Å}$ (41 eV), He I $\lambda 584 \text{ Å}$ (21 eV), and Ly α

$\lambda 1216\text{\AA}$ (10.2 eV) to an acceptable level, while maintaining a high transmission in the telescope bandpass. The sharp absorption edges of the filters at shorter wavelength (182 eV for Lexan/B, and 73 eV for Al/C) will also reduce the contribution of higher-order reflections from the LSM mirrors. Using previously established techniques (Vallerga *et al.* 1986), we anticipate using Lexan/B and Al/C filters with thicknesses of 2000 \AA , 1000 \AA and 1500 \AA , 700 \AA respectively. The peak transmissions are ~ 0.35 for Lexan/B and ~ 0.30 for Al/C. We have also found (Vallerga *et al.* 1986) that these types of filters will attenuate the low-energy charged particle flux by many orders of magnitude, helping keep down the detector background.

4. BACKGROUND CONSIDERATIONS

Backgrounds in the ALEXIS detectors can come from scattered sunlight, cosmic ray and trapped particles, and intrinsic radioactivity. These backgrounds must be minimized to not saturate the telemetry and optimize sensitivity. The particle background is minimized by the telescope geometry, since there are no straight-line vacuum paths to the detector from outside the spacecraft. The aperture is restricted and can be covered by magnetic fields that sweep away electrons. Scattered sunlight is rejected by the mirror and filters. Intrinsic radioactivity is minimized by proper choice of detector materials (see above).

Low-energy electrons are the most numerous of background-producing agents in low earth orbit (LEO) and geosynchronous orbit (GEO); ALEXIS will fly in LEO but is designed to reject electron backgrounds in both orbits. In an ALEXIS telescope, a low-energy electron coming through the aperture must scatter or produce secondaries before it can interact with the detector. Electrons incident on the mirror create secondary photons, mainly Si K- α (1.8 keV), Si L-lines (0.09 keV), Mo L-lines (2.5 - 2.9 keV), and Mo M-lines (0.4 - 0.5 keV). The higher the photon energy, the greater the depth into the mirror from which secondary radiation can escape. Beyond some depth, fluorescent secondaries are reabsorbed before they can escape the mirror. Integration of electron energy loss, secondary production, and secondary radiative transfer over our Mo-Si LSM mirror and quartz substrate shows that for an incident electron spectrum typical for GEO (Fritz *et al.* 1977), most background counts arise from electrons in the range 5 keV to 50 keV. If the GEO electron spectrum passed unimpeded through the aperture, the background rate would be about 50 counts s^{-1} from Si K- α alone. Mo L-lines account for about 1/4 as many, and Mo M lines about 1/10 as many background counts as Si K- α . Therefore, these electrons cannot be allowed to strike the mirror. Photon secondaries from proton and alpha particle impacts on the mirror produce negligible background counts.

Fortunately, low-energy electrons can be rejected efficiently by magnetic fields at the aperture, far from the mirror. Kilogauss fields are obtained with an arrangement of permanent magnets, such that field is concentrated at the aperture while remaining less than a gauss a few inches away (the drift region between MCP and anode is extremely sensitive to stray fields; conceivably, spacecraft attitude could be perturbed by magnetic torques also). We believe a thin, eight-piece quadrupole magnet around the aperture with a high-permeability disk in the (occulted) center of the aperture will provide sufficient field. Stray fields are minimized if the dipole moments of the eight magnet pieces cancel to high precision. Fringe fields on the inner plane of the quadrupole can be "clamped" with a thin mu-metal shield, and the detector interior will be shielded by a mu-metal can. This arrangement rejects electrons of 300 keV and less or deflects them into telescope baffles far from the mirror.

The thin filter at the detector serves as a final barrier to very low-energy particles (e.g., electrons below a few kilovolts) that elude the magnetic sweepers (e.g., by being created inside the telescope). In addition, the filter and front of the detector are biased negatively with respect to ground, preventing electrons below 4-5 keV from ever reaching the filter.

High energy electrons (those above 1 MeV) cannot be rejected completely at the aperture. If they strike the inner surfaces of the telescope and produce secondary photons or electrons, background counts can be produced. We are currently studying this problem using Monte Carlo transport calculations. A system of baffles will be incorporated on inner surfaces of the telescope tubes, outside the volume through which good photons pass, to minimize these possibilities.

Scattered sunlight produces intense photon backgrounds in the extreme and far ultraviolet. These photon backgrounds are controlled with in-line filters in front of the detector and by the wavelength selectivity of the mirror. Scattered solar Ly α ($\lambda 1216\text{\AA}$) I.E.O. is 25,000 Rayleighs even in the antisolar direction, so filters must be very efficient in rejecting it (1 Rayleigh = $10^{16}/4\pi$ photons $\text{cm}^{-2}\text{s}^{-1}\text{sr}^{-1}$). If unfiltered, the Ly α background could yield millions of counts per second. Scattered solar He II 304 \AA emission, typically 1-2 Rayleighs except at flare times,

Earth's shadow, is also a potential background source, but the low mirror reflectivity (see section on LSMs) keeps this contribution to the background under control.

5. FRONT-END ELECTRONICS WITH HIGH DYNAMIC RANGE

The front-end electronics must sense and ratio the wedge, strip, and zig-zag signals to yield the position of photons and bursts of photons at the front of the microchannel plate. This must be done over a dynamic range of 10^4 , ranging from single photon events that yield 10^7 electrons on the anode, to burst events that yield 10^{11} electrons. In each case, positions are calculated via the formulae $x = Q_W / (Q_W + Q_S + Q_Z)$ and $y = Q_S / (Q_W + Q_S + Q_Z)$, where Q_W , Q_S , and Q_Z are the charge collected by the wedge, strip, and zig-zag anodes, respectively. To accurately ratio events over such an extreme range requires a unique low-noise front-end design.

To properly sample the telescope point-spread function, we require a spatial resolution of 1.128 over the 40 mm field-of-view (thus $\sim 300 \mu\text{m}$ FWHM). Meeting this requirement takes an A/D converter with a dynamic range of $10^4 \times 3 \times 128$ (~ 22 bits); the factor of 3 is included to cover the variation of the charge ratios over the surface of the wedge-and-strip anode. The preamplifier must be wide-band to match detector rise times of 1 nsec. In order to cover this large dynamic range with a modest A/D converter (12-bit), the range is split equally into two ranges (100x different in sensitivity) by switching the gain at the preamplifier. Both the lower and upper range will give a dynamic range just over 10^2 , with the lower range covering events from modal ($10^7 e^-$) to 240 times modal.

6. DATA HANDLING AND EVENT POSITION CALCULATION

The ALEXIS payload data processing unit (DPU) is a multiprocessor system that includes four 80C86 microprocessors, organized as shown in Figure 5. The DPU has the task of calculating event positions from the digitized wedge, strip, and zig-zag anode signals, and processing event data (for example, compressing the event stream) before it is sent to the telemetry stream.

From the point of view of the DPU, the ALEXIS payload is seen as three identical telescope-pair units. Each telescope pair is associated with analog electronics, an 80C51 microcontroller, an independent 80C86 processor system, and high and low voltage power supplies. These three detector and data processing units are governed by a fourth 80C86 processing system that acts as the payload data handler, performs data compression, detects and corrects errors, arbitrates tasks, and interfaces to the spacecraft electronics. The four processing systems communicate with each other over a global data bus using a shared global memory. A dual-port memory allows two-way communication between the payload system and the spacecraft's independent processing system (the spacecraft processing system also contains at least one microprocessor, bringing the total number of on-board microprocessors and microcontrollers to at least eight).

Within each telescope-pair unit, the 80C51 acquires three channels of detector data (wedge, strip, and zig-zag amplitude) for each photon event. It then records the time of each event, packs the data into a message and transmits the message serially to its dedicated 80C86 processor. The 80C51 also periodically gathers housekeeping data, packs these data into a message, and transmits this message as well.

The 80C86 processor system accepts messages from the microcontroller and processes the data that they contain. Processing activities include mapping the detector data into two-dimensional points in the telescope's field-of-view. Processed data from each processing system are placed in global memory. From global memory, the data are formatted by the data handler processor into blocks into which error detection and correction (EDAC) blocks are added, and sent to the spacecraft processor through the dual port memory. The spacecraft processor stores the data blocks in mass memory until it is possible to relay the data through the RF interface to the ground.

Each dedicated 80C86 is a stand alone processor system with 128 Kbytes of electrically erasable, programmable, read-only memory (EEPROM) for program storage, and 512 Kbytes of RAM used for local data storage. The four payload 80C86's run identical copies of the operating code. This allows the function of the data handler processor to be assumed by one of the other processors, with some degradation in performance, if the normal data handler processor fails.

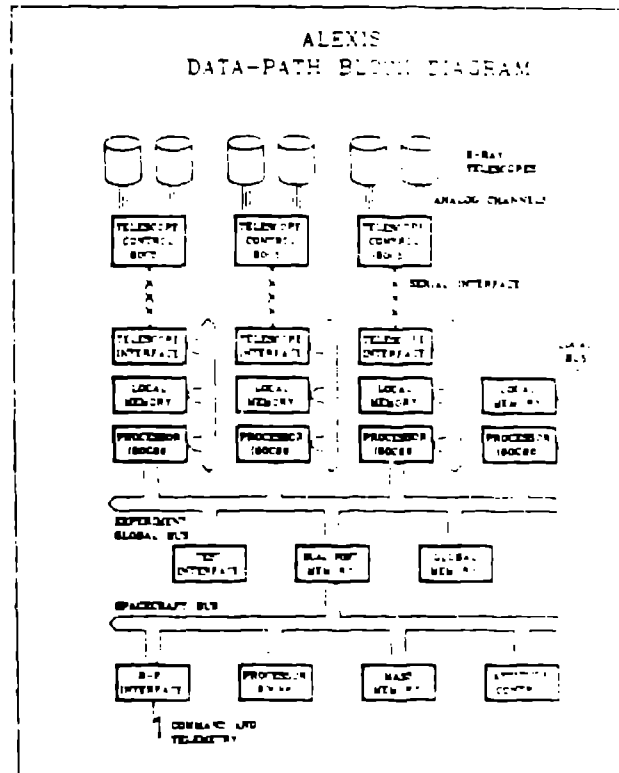


Figure 5. Block diagram of ALEXIS data processing unit (DPU).

All hardware is radiation tolerant to 10 krad (Si) minimum, consistent with a 3-year life in any low Earth orbit of up to 400 nm altitude. Hardware is also protected against single event upset (SEU) latchup. Extensive protection against single event upset in the memories and processors is being designed into both hardware and software.

7. COMPATIBILITY WITH MINISAT CARRIER: EXPERIMENT ENVELOPE

Figure 6 shows the ALEXIS experiment packed in a 21" x 22.5" diameter cylinder, sized for a miniature satellite that could be launched as a paired payload by a Scout or Pegasus expendable booster. ALEXIS stretches the envelope of past miniature satellites (Fleeter 1988), by extending the requirements for power, data storage, and telemetry in an evolutionary way.

To support the ALEXIS experiment, the minisatellite bus must provide the following resources:

- 100 pound payload capability
- 40 watts of unregulated 18 V power
- 10 kilobits/sec telemetry, orbit-averaged
- 100 kilobits/sec interface from experiment to spacecraft
- Aspect solveable to 1/4° (worst case)
- Spinning at 1-2 rpm, experiment anti-Sun pointed
- Operation from a single ground station at Los Alamos

Glossey photo
enclosed

Figure 6. ALEXIS experiment mockup. Only one telescope is shown for each pair. The experiment spin axis is vertical in this model.

The telemetry requirement is most easily met by a store and dump system. Continuous data are stored in an on board memory of 0.75 gigabit (static RAM), then dumped in passes over an experimenter ground station. For typical orbit coverage, the telemetry downlink must be of order 0.75 Megabit/sec.

8. GROUND SUPPORT HARDWARE AND SOFTWARE

The philosophy of low cost "Cheap-sat" technology carries over to the Ground Support Equipment (GSE), ground station, and data analysis system for the ALEXIS project. Providing one's own ground station and analysis capability represents a significant cost savings over the use of government or commercial space tracking services. By sharing as many components as possible between the GSE and the ground station as well as by adapting existing software packages for some of the data

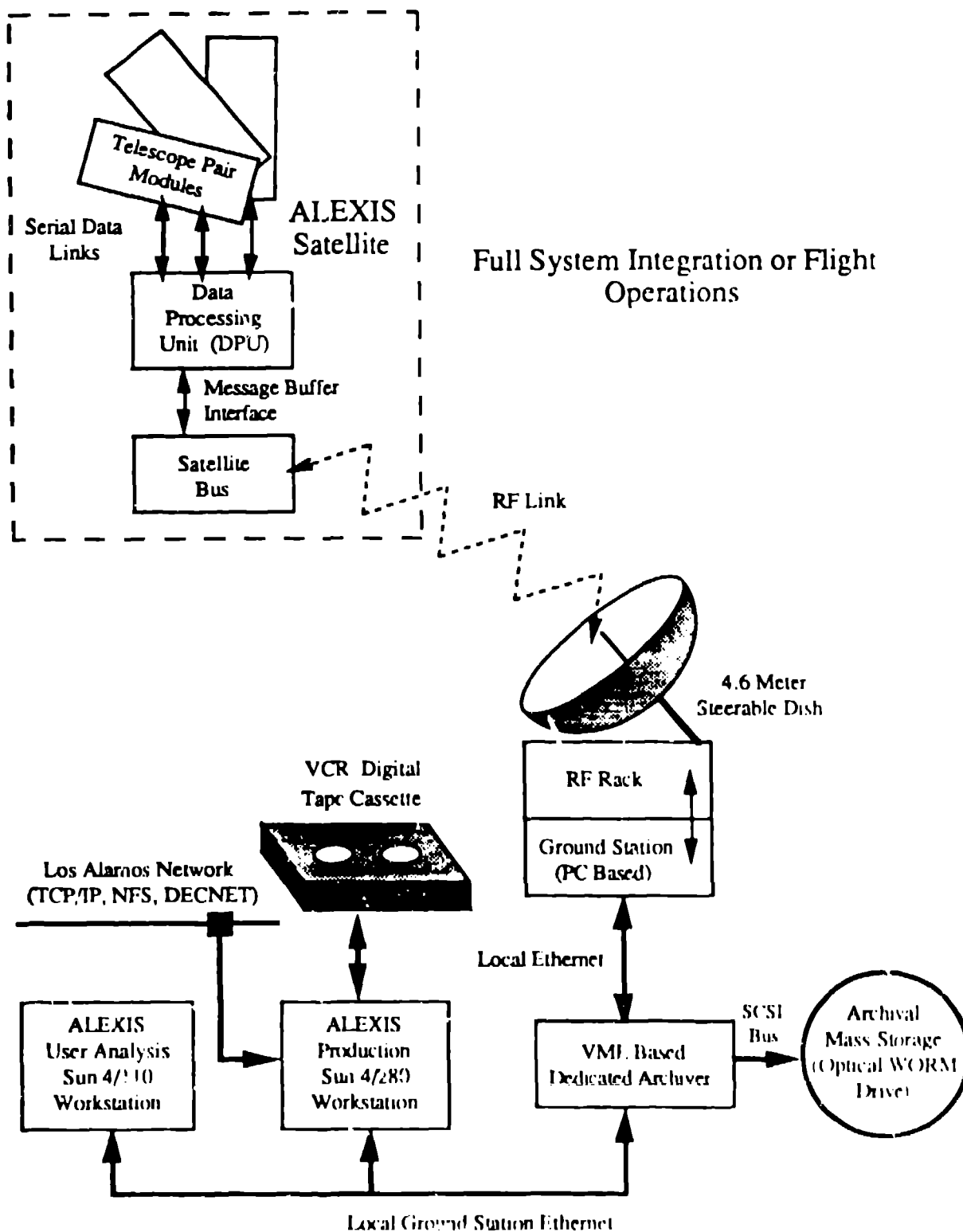


Figure 7. ALEXIS GSE as configured for flight operations

analysis we can reduce costs even further. Individual GSE components are provided by the team member building the related pieces of flight hardware. All of the different GSE units will communicate with each other via an industry standard bus.

8.1 Ground Support Equipment (GSE)

The ground support equipment will undergo a series of transformations as instrument development progresses from individual box test to full system integration and flight operations. Figure 7 shows the GSE as configured for flight operations.

As described previously, a pair of telescopes will share an electronics module containing a microcontroller. The same Sun scientific workstation will be used for all phases of ground test and flight operations. When a telescope is being calibrated in the laboratory, it will communicate via the microcontroller's serial data link to a VME-bus based single board computer (OIC). The OIC will perform the task of actually collecting data from the telescope, formatting the data the way it will appear in the telemetry stream, and passing it via an ethernet link to the Sun workstation. During integrated ground tests or actual flight operations, telemetry is transferred to the Sun workstation via ethernet. Using an industry standard interface like TCP/IP ethernet reduces the cost of assembling support modules due to the availability of compatible off-the-shelf equipment and components.

The analysis software in the Sun workstation will be independent of the data source. Portions of the analysis procedures on the Sun workstation will utilize the IRAF data analysis system supported by the National Optical Astronomy Observatories. This package is a general purpose image and data analysis system with a UNIX-like user interface. Custom user programs can be easily integrated into the system. Because IRAF runs on many different computer architectures, high level analysis of ALEXIS data will be available at several locations. We are also using the software package MONGO written by John Tonry at MIT for graphics displays. Both of these packages are inexpensive compared with commercially available software with similar capabilities. They are especially cheap when compared with the costs of writing similar code for ourselves. The software for the OIC used to collect data from the telescopes in the laboratory is to be written in C under a UNIX-like operating system kernel. Programs for the OIC will be written on the Sun and then downloaded via the ethernet link. This will allow us relatively rapid software development for the OIC.

8.2 Flight Operations

Flight operations will be run directly from Los Alamos, using our own tracking dish, an RF station provided by the satellite vendor, and workstations provided by Sandia and Los Alamos. We therefore have no requirement for TDRSS or tracking network services. Software for satellite tracking will be provided by the satellite vendor, software to monitor housekeeping data, grab the data stream, and generate commands will be provided by Sandia, and data acquisition and analysis software will be provided by Los Alamos.

During flight operations, a PC-based GSE provided by the satellite vendor will track ALEXIS with a 4.6 meter dish during a pass and transmit commands. Initial operations of the spacecraft, as it is configured for experiment turn-on, will be controlled by the satellite vendor. When the experiment doors are opened, operations will be handed over to Los Alamos. Commands will be generated and checked at the Los Alamos ground facility, then uplinked to the spacecraft. In early operations, Los Alamos will provide 24-hour support of ground passes; later, we hope to automate the process by storing commands and pre-programming data acquisition. UCB/SSL will support flight operations as required per their role in providing detectors; in particular, they will be present at the ground station during initial instrument turn-on. Their role in the ongoing flight data operations is detailed below.

These do-it-yourself flight operations are possible because ALEXIS operates in a single, spinning survey mode. The experiment need not be commanded on a regular basis. Our observation schedule is fixed by the spacecraft spin and the annual motion of the Sun around the sky; we need not schedule or command observations of individual sources.

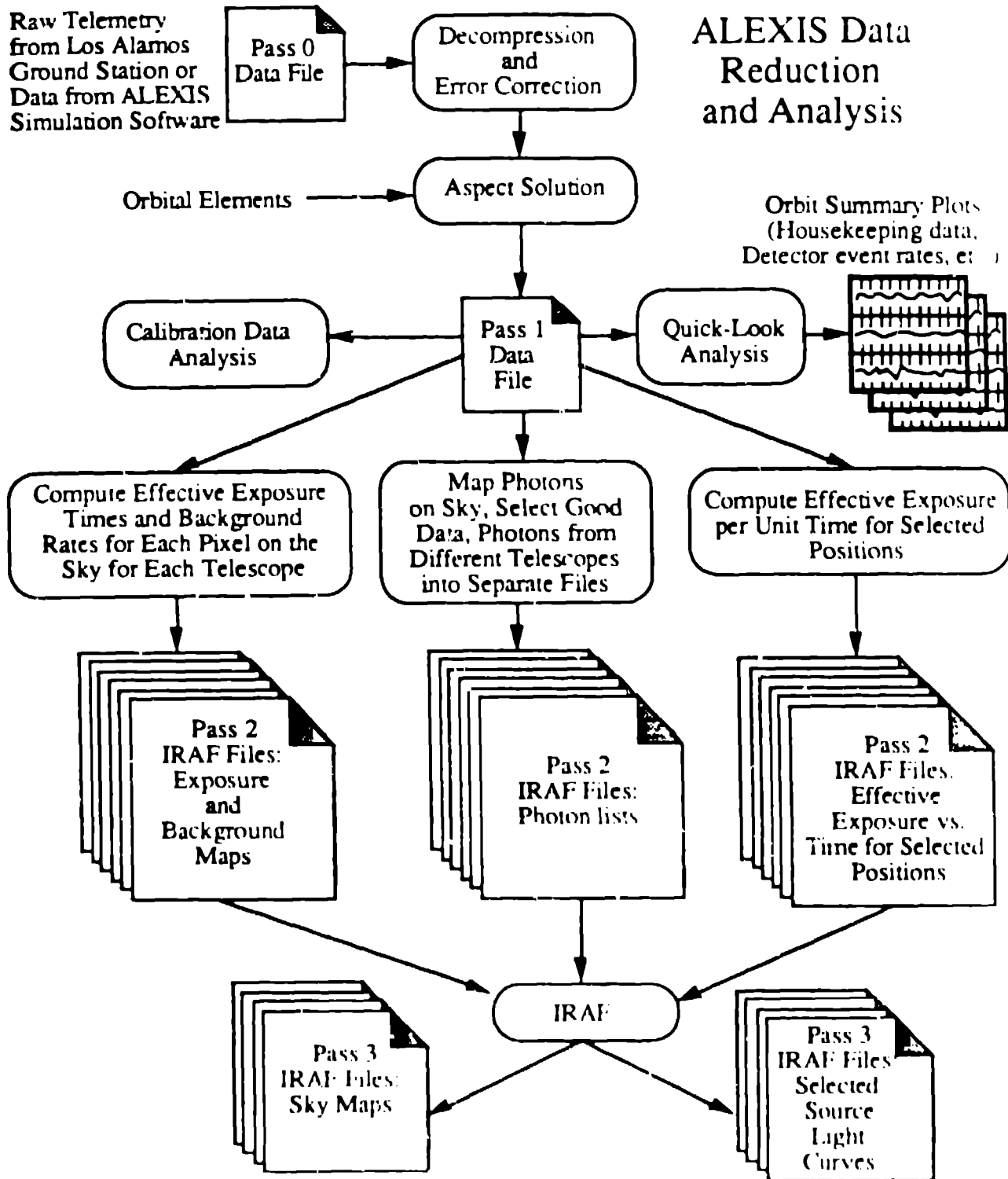


Figure 8 ALEXIS data analysis flow chart

8.3 Data Analysis Software

The analysis of ALEXIS data will be patterned after the EUVE End-to-End System (EES), being developed at UCB. The ALEXIS analysis software will produce diffuse background maps as well as catalogs and light curves for sources in the ALEXIS data base. The data flows from a satellite-specific front end that solves aspect, computes UTC times, corrects for detector distortions and assigns the results to individual photon events in the telemetry stream (see Figure 8). Further reduction will be handled with software installed in the IRAF (Image Reduction and Analysis Facility, developed by NOAO at Kitt Peak National Observatory). The unique satellite-specific software will be developed at Los Alamos, while the IRAF analysis routines will be developed at UCB in consultation with Los Alamos as part of the EUVE EES program. For example, methods for detecting and measuring point sources and timing analysis will be installed in IRAF. A data base system will also be developed to minimize the time required to access reduced data on a given portion of the sky. Maps of diffuse sky emission in the different telescope bands will also be stored and analyzed within IRAF.

9. SCIENTIFIC OBJECTIVES AND SENSITIVITY

9.1. The Value of an Emission Line Survey

ALEXIS is aimed squarely at mapping the sky and monitoring point sources in certain strong emission lines. Its combination of narrow-band ultrasoft X-ray spectral response and roughly 1-degree spatial resolution has never been flown as a sky-survey instrument.

Historically, spectroscopy has been the prime tool for remote diagnosis of plasmas, providing measurement of temperature, density, and elemental abundances for sources at great distance. Before stellar spectroscopy was developed, for example, it was thought that the composition of stars would never be known. Afterwards, astrophysics could begin as a science. Objective prism surveys quickly showed spectra of hundreds of stars. Spectral classification systems followed, while the composition of stars, along with many other revelations, was elucidated by spectrophotometry of ever-increasing sophistication. Exciting objects, such as SS 433, have been found in emission-line surveys in the optical band. Spectroscopy of the gas between the stars has been equally rewarding. Photography of the sky through highly selective interference filters (e.g. Parker, Gull, and Kirshner 1979) has produced dramatic images of filamentary structures of supernova remnants connected over many degrees.

Spectrophotometry in the X-ray band has been rewarding. In the early years of X-ray astronomy, several types of sources were thought to generate X-rays through nonthermal processes associated with cosmic rays. Exotic models were created to explain X-ray emission from supernova remnants and clusters of galaxies. These models had to be discarded after strong, narrow atomic emission lines were found in their spectra, firm evidence that the emission mechanism was thermal emission from hot plasmas.

The diffuse soft X-ray background is expected to show a highly structured line spectrum. Thermal emission from a hot plasma is the favored hypothesis, not due to discovery of narrow emission lines, but due to the elimination of other possible origins. There is one observation to date of oxygen line emission from the diffuse background, apparently from interstellar gas (Inoue et al. 1979), but the thermal nature of the emission remains to be conclusively proven.

Figure 9 shows contours of emissivity coefficient for a hot plasma in coronal equilibrium with normal cosmic abundances (Raymond and Smith 1977). The temperature range is 10^5 to 10^7 K, typical for plasmas in interstellar space and the coronae of stars. There are no strong emission lines above 75 eV. Below 75 eV are several very strong lines. In particular, there are lines around 72 eV from Fe VIII, Fe IX, Fe X, and O VI that fall in the lowest energy ALEXIS band. Figure 9 graphically shows the predominance of ultrasoft X-ray emission lines under interstellar and coronal conditions.

Since most of the radiation from hot plasmas in the temperature range 10^5 to 10^7 K is contained in emission lines, an experiment sensitive primarily to emission lines, i.e. ALEXIS, has the best chance of observing structure in the diffuse background. The images gathered by ALEXIS should be analogous to the interference filter images of interstellar structure obtained in the optical band, although with poorer angular resolution.

The sun is a bright source of emission lines in the ALEXIS bands. In particular, photographs of the sun in a bandpass similar to the ALEXIS 72-eV band have been obtained recently on a rocket flight (Walker et al. 1988). Adding up the total intensity of various lines, it turns out that ALEXIS can only detect the Sun's corona out to 2 pc. However, many stars are far more active than our sun, and we expect to observe many extrasolar coronal systems.

In summary, ALEXIS, by mapping the sky in several narrow emission line bands, will have a unique capability to identify point sources with strong thermal emission and map the diffuse ultrasoft X-ray background.

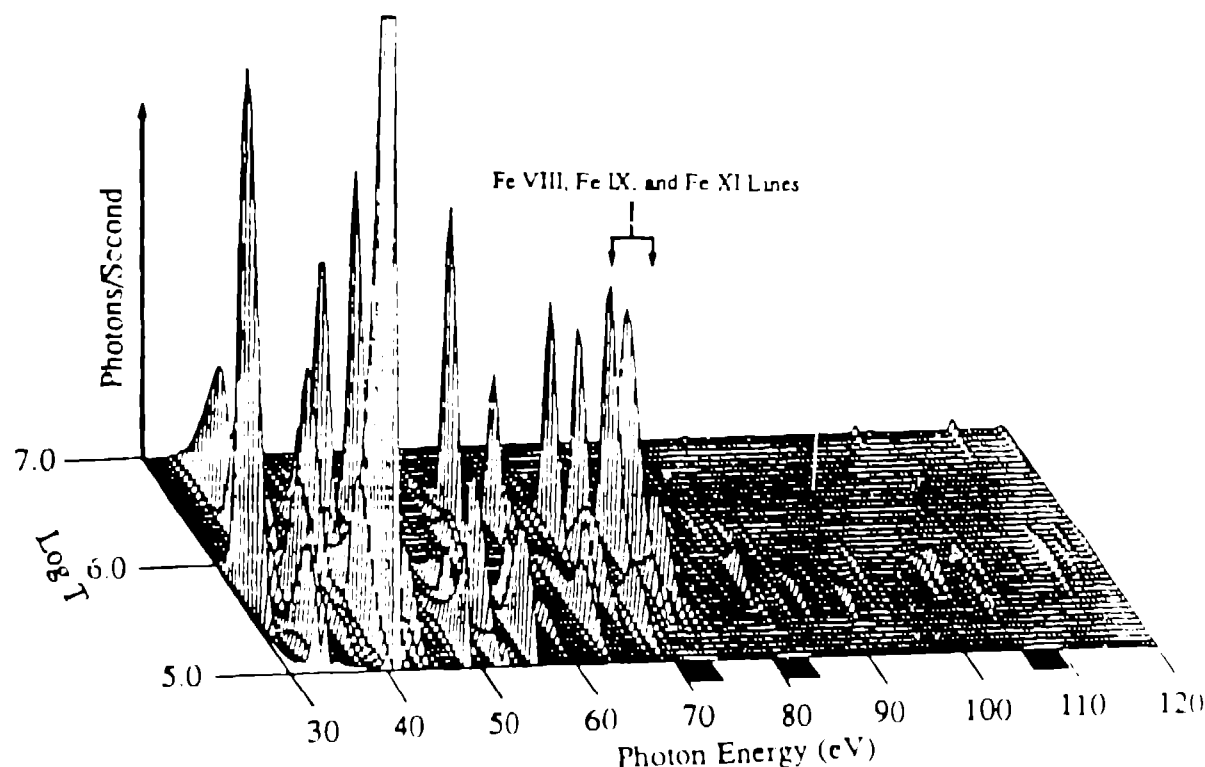


Figure 9. Emission from a hot, coronal plasma, as a function of temperature and wavelength.

9.2 ALEXIS Instrument Sensitivity

We have made preliminary calculations of the sensitivity of the individual ALEXIS telescopes. Predictions of the LSM mirror reflectivity, in combination with data for the transmission of filter materials and the quantum detection efficiency of MgF_2 opaque photocathode material were used as input data. Code developed for predicting the minimum detectable flux for the EUVE mission was adapted for this purpose.

MgF_2 is used to enhance the quantum detection efficiency while retaining good photocathode time stability. The thin film filters will be placed in front of the detectors to exclude the intense photon flux outside of the mirror bandpass due to the strong geocoronal background. Even though ALEXIS is insensitive to the brightest geocoronal lines ($\text{He II } \lambda 304\text{\AA}$, $\text{He I } \lambda 584\text{\AA}$, and $\text{Ly } \alpha \lambda 1216\text{\AA}$), they are still so bright as to completely dominate the background count rate. Were it not for the filters, $\text{Ly } \alpha$ would swamp the detectors with more than 10^6 cts/sec. We have chosen as candidate filters Lexan/Boron and Aluminum/Carbon, with broad bandpasses centered at ~ 120 eV and ~ 70 eV, respectively. This choice is based on previous experience and measurements in the development of filters for the Extreme Ultraviolet Explorer (EUVE) (Vallerga et al. 1986). Lexan/Boron will be used for the high energy bandpass telescopes (85 eV and 107 eV) and Aluminum/Carbon for the low energy bandpass (72 eV). The filter thicknesses are optimized to reduce unwanted background while retaining high throughput in the telescope bandpass.

We must also minimize far UV leaks that would lead to false detections of bright EUV sources like O and B stars. Material constraints are also included in the optimization: can the filter be made and launched and will it remain stable?

Once an optimized filter has been chosen, the sensitivity of the three ALEXIS bands can be calculated given the background rates, the exposure time and the instrument throughput. The "strawman" filter design (Lexan/Boron - 2000Å/1000Å thickness; Aluminum/Carbon - 1500Å/700Å thickness) gives the following night sky background rates: 31 cts/sec in the 72eV band (dominated by 304Å flux); and 10 cts/sec in the 85 and 107eV bands (dominated by detector background). These rates do not include the counts due to the diffuse soft x-ray background (SXRb) that ALEXIS has been designed to measure. For example, the 72eV band count rate would increase to 89 cts/sec if all the SXRb measured by previous experiments were due to the Fe VII-X line cluster at 72eV. This would be considered a best case for measurement of the SXRb or the worst case for the point source sensitivity calculation. In the following calculations of point source sensitivity we have assumed that the SXRb does not dominate the telescope backgrounds, but we have been conservative in our estimate of geocoronal background, mirror reflectivity and telescope imaging.

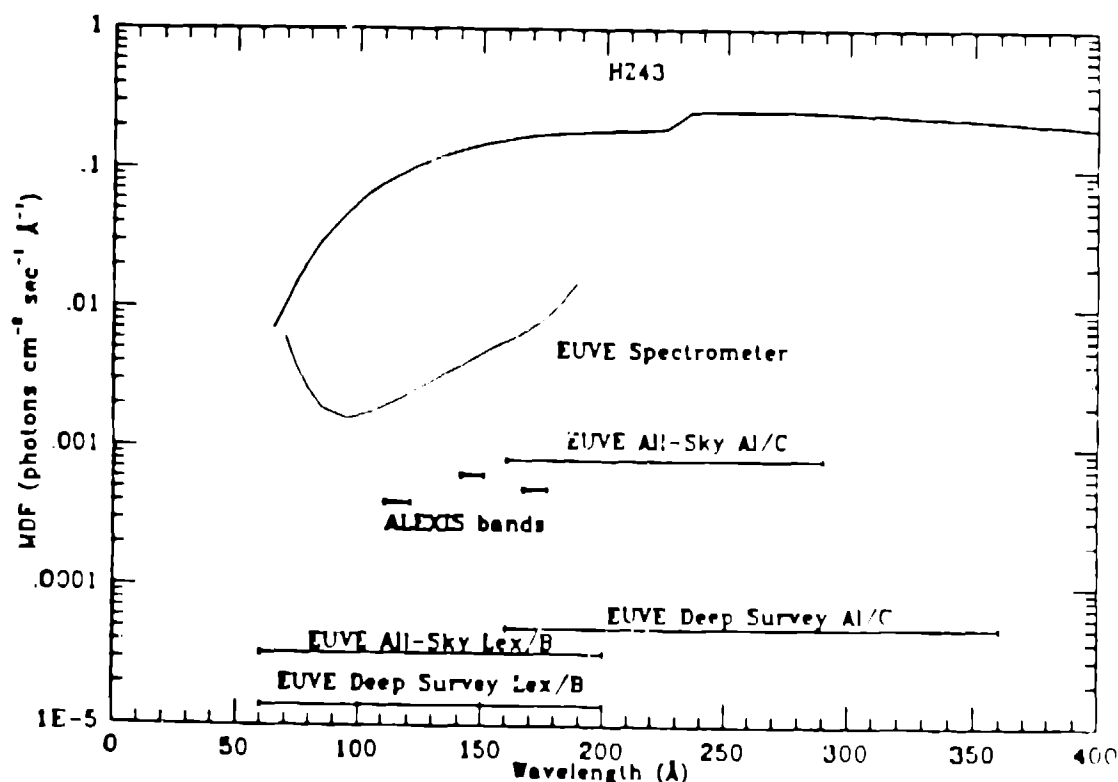


Figure 10 ALEXIS Sensitivity to Continuum Sources (6 month exposure)

In six months, each telescope will have a mean exposure per source of 120,000 seconds (nighttime only, though calculations show daytime operation is feasible, especially for the shorter wavelength bands). With an effective image diameter of 1°, this yields a minimum detectable flux (5σ) for a line at the center of the band of 8×10^{-3} photons $\text{cm}^{-2} \text{s}^{-1}$ (72 eV), 9×10^{-3} photons $\text{cm}^{-2} \text{s}^{-1}$ (85 eV), and 4×10^{-3} photons $\text{cm}^{-2} \text{s}^{-1}$ (107 eV). Observations with a 1-day time resolution will have about 10 times the minimum detectable flux stated above. Sensitivity to continuum sources (Figure 10) can be estimated from these line flux sensitivities by dividing by the effective bandwidth of each mirror.

The telescopes pointing in the direction of the spin axis observe a strip $\pm 30^\circ$ about the ecliptic plane since the field of view is offset from the spin axis by 10° . This strip gets twice the average exposure of regions 90° from the spin axis. In the most favorable regions, the exposure peaks at 1.6×10^6 sec, improving the sensitivity in this region by a factor of four, and increasing the expected number of observable sources by a comparable factor. We

consider the sensitivity numbers above a conservative estimate, and expect that they will improve as we refine the filter and mirror design of ALEXIS.

9.3 Soft X-Ray Background and Old Supernova Remnants

The soft X-ray background (SXRb) emission (70-250 eV) is thought to originate in a $\sim 10^6$ K plasma that fills the local interstellar medium. Figure 11 shows a map of the SXRb in the B band (130-188 eV) in zero centered galactic coordinates (McCammon *et al.* 1983). Equilibrium emission models of an optically thin, million-degree plasma with normal cosmic elemental abundances predict that 34% of the atomic cooling power comes from a set of closely-spaced lines around 72 eV from Fe VIII, Fe IX, and Fe X. Radiation from these lines in the SXRb has yet to be unambiguously measured. These lines should have dominated measurements of the SXRb in the Be band (70-110 eV; see Bloch *et al.* 1986), but pulse-height analysis of the Be band data yields a mean energy which is incompatible with intense 72 eV emission (Bloch 1988). The flux from the Fe lines must be reduced by approximately a factor of 10 with respect to the rest of the SXRb spectrum within the Be band to make the model spectra compatible with the observed pulse height distribution. One way that the broad band Be, B (130-188 eV), and C (160-284 eV) band rates can be reconciled with the Be band pulse-height distribution is to use a plasma emission model with depleted heavy element abundances, as exists in the neutral component of the interstellar medium. Such a situation might arise if the hot plasma was formed by heating cool gas that contained dust, if the dust has not yet been evaporated by the hot component. The depletion of Fe and other refractory elements has considerable effect on the cooling power of interstellar gas. Depleted gas is nearly an order of magnitude less effective in radiating its heat at 10^6 K, with a corresponding impact on the inferred density of the hot interstellar medium.

A direct measurement of the flux in the 72 eV Fe lines would provide an important diagnostic of the hot local interstellar medium. The ALEXIS telescopes would be tuned to 72, 85, and 107 eV to map the Fe VIII-X cluster, O VI (82.6 eV), and Ne VII (106.25 eV) / O VI (107.07 eV), respectively. Counts in the 72 eV bandpass would range from a few to ~ 100 counts sec^{-1} per telescope, depending on the composition and temperature of the SXRb gas. With the narrow response of these bands ($\sim 5\% \Delta E/E$), the flux in these lines could be unambiguously measured. After one year of observations, we expect to achieve 5σ sensitivities of 2-6 photons $\text{cm}^{-2} \text{sr}^{-1} \text{sec}^{-1}$ on a 1° scale. These maps will far exceed previous maps of the SXRb in angular resolution (previously 3°) and spectral selectivity (previously $\Delta E/E \sim 1$). For example, previous maps have had resolutions of 3° in the C-band, 6° in the B band, 15° in the Be-band, and do not exist at lower energies. From the ALEXIS maps, one will be able to resolve previously ill-defined features such as a possible connection between the North Polar Spur (a nearby old supernova remnant?) and the local bubble. In combination with multi-wavelength data from other instruments such as the Diffuse X-ray Spectrometer experiment we hope to gain a better understanding of the dynamics, history and composition of the hot component of the local ISM.

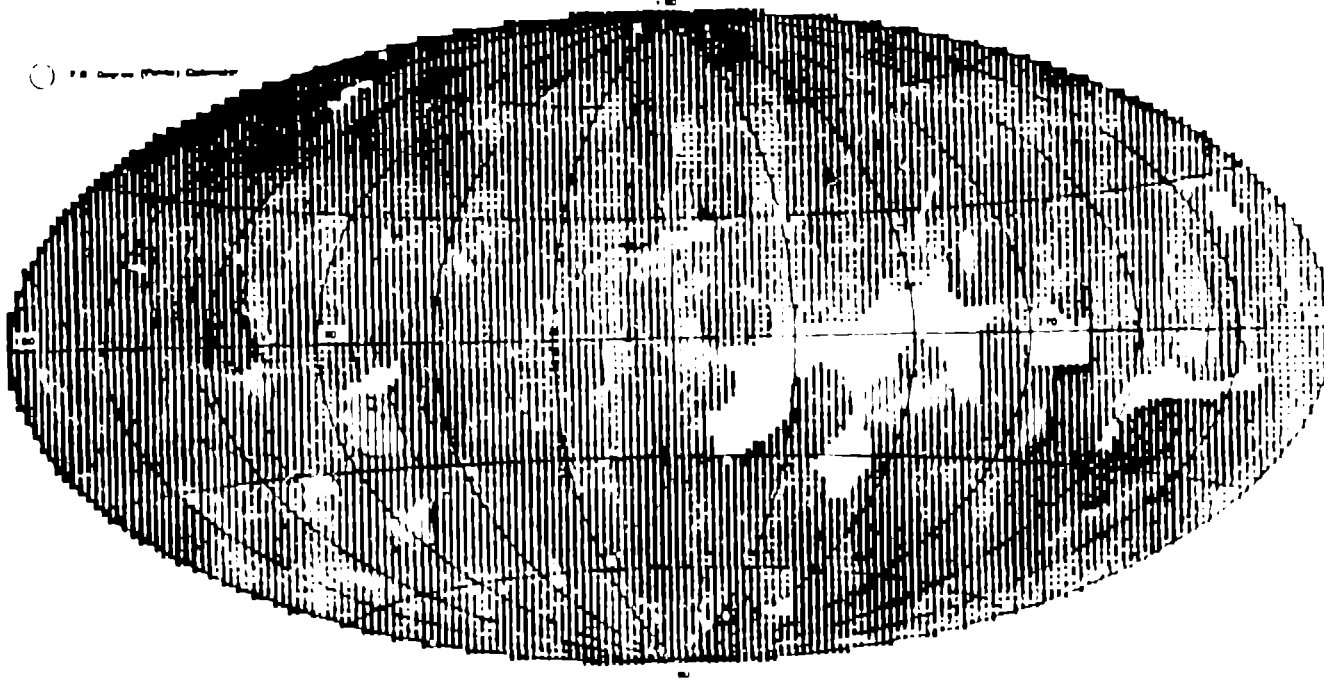


Figure 11. Map of the diffuse soft X-ray background (130-188 eV).

9.4 Narrow Band Survey

Narrow Band Photometry: Figure 10 shows the relative sensitivities of the ALEXIS narrow bands and of the telescopes on the Extreme Ultraviolet Explorer (EUVE). This plot demonstrates the potentially strong tie between the data obtained by the two instruments. Although EUVE will reach fainter sources in the all-sky survey, the survey yields very little spectral information. The main reason for this is that many objects will be limited at long wavelengths by the absorption due to cold hydrogen along the line of sight. Detection in the shortest band (at about 100Å) will only occasionally be accompanied by a detection in the next longer wavelength filter (at about 200Å). ALEXIS can provide three data points along the spectral energy distribution for many sources detected in the EUVE all-sky survey (effective resolution $R \approx 15-20$).

We may estimate the total number of objects for which these measurements are possible. The ALEXIS limits are about a factor of 10 larger than the EUVE sensitivity at 150Å. The source number flux relation is usually parametrized as $N = K S^{-\alpha}$, where α can be between 0.5 and 2.5, depending on the geometry of the source population. A Euclidian distribution of sources gives $\alpha = 1.5$; a disk population gives $\alpha = 1.0$, while a class of sources that is limited by the absorption due to the ISM can give $\alpha = 0.5$. If $\alpha = 1.0$, ALEXIS would be able to detect about 10% of all the sources in the EUVE catalog. Thus, we would be able to measure or place constraints on the spectral energy distribution of many classes of EUV source (see below).

The EUVE Spectrometer performs a complementary function by obtaining higher resolution ($R \approx 200-500$) spectral data for a fraction of the sources in the EUVE all-sky survey. The ALEXIS sensitivity to continuum sources (or broadened and/or blended emission lines) is 5-10 times better than the EUVE spectrometer, but 2-4 times worse for sources whose spectra consist primarily of a few narrow lines. Furthermore, the EUVE spectrometer can be used in pointed mode only, while ALEXIS will examine the entire sky. It has been estimated that only 30-100 objects may be observed spectroscopically by EUVE in one year, while the survey may detect nearly 10,000 sources, of which 1000 could be measured by ALEXIS.

Cool Stars: The ALEXIS experiment will make unique and valuable contributions to the study of the transition regions and coronae of cool stars. Observations with the *FUSE* Observatory demonstrated that the

of all spectral types (with the possible exception of A stars and supergiants) are soft X-ray emitters (Maggio *et al.* 1987; Schmitt *et al.* 1985; Golub *et al.* 1983; Rosner *et al.* 1981). Of the serendipitous sources detected by EXOSAT, 75% were stars (Giommì, Tagliaferri, and Angelini 1988).

Estimates show that there are ~4500 main sequence stars of spectral types F, G, K, and M out to a distance of 25 pc (Allen 1973). Given the typical soft X-ray luminosities of these stars and the sensitivities of the ALEXIS detectors, ALEXIS will be able to observe cool stars out to ~15 pc. Based upon these numbers, we predict that a few hundred main sequence stars as well as ~1 to 5 nearby RS CVn type stars will be detected in the ALEXIS survey.

The bulk of the soft X-ray emission from these stars originates in plasma material at temperatures between 10^6 and 10^7 K in the coronae of these stars. Stellar coronae are believed to contain plasma which is not simply isothermal, but rather has components which span a continuous range of temperatures, including components that radiate strongly in the ALEXIS bands.

Early Type Stars: Early type stars are another class of Galactic objects which emit ultrasoft X-rays (Lora and White 1980). There are a large number of nearby O and B type stars which will be detectable with ALEXIS, such as the bright stars α Vir, β Cen, α Leo, and α And. Of the 380 stars detected serendipitously with EXOSAT, the vast majority were early type stars (Giommì, Tagliaferri, and Angelini 1988); fully 200 alone were B stars. The EXOSAT instruments did have substantial portions of their bandpass in the X-ray region (> 250 eV), so the detected flux from early type may be largely due to X-ray emission. But the sheer numbers of O, B and A stars found by EXOSAT strongly suggests that ALEXIS will detect many of these objects. By comparing the measured fluxes with UV and optical data, possible mechanisms for the emission can be discerned.

Currently, there are two competing models for the soft X-ray emission from early type stars: the "coronal slab" model and the "shocked wind" model. The favored shocked wind model postulates that hot shocks are generated in radiatively driven winds; the shocks then produce the observed soft X-ray emission. In the coronal slab picture, X-rays emitted at the base of the stellar wind ionize material in the wind to produce the soft X-rays. Measurements of the soft X-ray fluxes from early type stars with ALEXIS will be beneficial in helping to distinguish between these two scenarios. It will also indirectly determine several of the parameters in the model, based upon the measured fluxes from early-type stars.

Flare Stars: Numerous nearby dwarf K and M stars are known to flare from time to time. These flares are usually many times brighter than flares on our own Sun, and the cause and emission mechanism are still not well understood (e.g. Haisch *et al.* 1981, Kahn *et al.* 1979, Heise *et al.* 1975). Only a few stellar flares have ever been observed in the ultrasoft X-rays, and observations with the ALEXIS satellite will add greatly to our knowledge of these objects.

The large field of view of the ALEXIS detectors and the rapid spin rate of the satellite mean that it will be an excellent monitor of sudden flaring activity on nearby stars. Because of the limited data currently available, the expected fluxes and flare rates in the soft X-ray regime are not known. Based upon the flare rates determined by Connors, Serlinitsos, and Swank (1986), though, and the sensitivities of the ALEXIS telescopes, it can be estimated that ALEXIS will detect between 8 and 25 stellar flares from nearby stars during a 6-month survey. The actual number of flares detected by ALEXIS will allow a much better determination of the flare rate distribution (log $N - \log S$) in the soft X-ray portion of the spectrum.

Coordinated optical, radio and X-ray observations of flare stars will be another important contribution from ALEXIS. Since ALEXIS views 1/2 of the sky during each satellite spin, it can monitor the ultrasoft X-ray emission from flare stars which are being observed from the ground by optical and radio astronomers. Flares from flare stars have typical durations of 100 - 1000 seconds, longer than a single spin duration of the satellite, so ALEXIS will not "miss" any flares while it is looking away.

The soft X-ray emission from stellar flares originates in plasma material in the coronal and transition regions at temperatures of 1 - 10 million degrees Kelvin. The narrow band fluxes measured by ALEXIS will provide sensitive determinations of the plasma temperatures and emission measures in the flaring material. Combined with the light curve information, this will aid in pinning down the mechanism behind the flare process on dMe stars.

Planetary Observations: ALEXIS might observe highly ionized species in planetary magnetospheres. The best candidate for detection is the Io torus, which contains ionized Na, K, S and O resulting from collisional

excitation of neutrals by magnetospheric electrons. To date, the most highly ionized species observed are S IV and O III at energies of 47eV and 55eV, respectively. However, there are several bright emission lines which could be detectable by ALEXIS. In particular, the emission lines of O V (172Å, 193Å) and O VI (173Å, 150Å) are strong features which should be observable if the densities of these ions in the torus is greater than a few ions cm⁻³. Detailed modeling of the Io torus suggests that during the Voyager spacecraft encounters the O V and O VI densities were less than this (Shemansky, 1987). However, the densities of the highly ionized species show large abundance variations that may be linked with vulcanism on Io. Other species which may be observable include S IV, Na IV and Si V.

Quasar Studies: Many experiments now indicate that there is a strong soft X-ray or extreme ultraviolet component in the spectra of nearby Active Galactic Nuclei (AGN) and quasars (Wilkes and Elvis 1987, Pounds 1988). The nature of this component is completely unknown (and its existence not predicted) but may be related to a large accretion disk surrounding a supermassive black hole ($M \sim 10^6$ - 10^7 solar masses; cf. Bechtold *et al.* 1987 and Pounds *et al.* 1986). The opacity of the interstellar medium limits potential sources to those lying along low column density lines-of-sight (Lockman *et al.* 1986). Very few quasars and AGN show significant intrinsic absorption (Wilkes and Elvis 1987). Based on similar calculations done for EUVE, we estimate that ALEXIS observations could detect 10-100 AGN and quasars if this emission is due to a thermal continuum from the disk.

Theories of accretion disks have predicted that matter is blown off the disk at large radii due to reheating by X-rays from the inner radii or heated plasma in magnetic flux loops (Shakura and Sunyaev 1973, Galeev, Rosner and Vaiana 1979). The heating is probably sufficient to form an optically thin wind at temperatures of 10^6 - 10^7 K (Bisnovatyi-Kogan and Blinnikov 1977). The resultant corona may be responsible for the soft X-ray excesses.

If the excess flux is primarily in emission lines, then ALEXIS would detect just as many sources but there would be a strong dependence on redshift. Detections at a limited number of discrete redshifts would then indicate that quasars have similar spectra as a class, dominated by individual plasma lines. One interesting possibility is that we could reconstruct the spectrum of typical quasars by combining data from objects at many different redshifts. Detecting quasars with $z = 0.3$ would result in a composite spectrum from 30Å to 170Å (72 - 430eV) at a resolution of 10Å. Broad absorption features in the quasar spectra due to the Carbon edge at 44Å (in the AGN rest frame) would also produce redshift-dependent effects that could be investigated with ALEXIS data by examining ratios of two adjacent narrow bands.

9.5 Relation to Broadband Surveys

There could be a profitable synergism between the EUVE and ALEXIS experiments. Many studies could be performed that would not be otherwise possible. For example, one may use the narrow band data for white dwarfs detected in the broad-band survey to determine interstellar column densities. White dwarfs may be detected in multiple ALEXIS bands if the interstellar hydrogen column is less than about 10^{20} cm⁻²; in contrast, only one EUVE channel will detect sources at greater than 2×10^{19} cm⁻². The band ratios will be sensitive to column densities greater than 1×10^{19} cm⁻².

Narrow-band data can be quite important for discriminating between possible physical models of the emission region. If the narrow-band fluxes are comparable to broad-band values, one may infer that the emission is primarily in the form of narrow lines, and probably due to an optically thin plasma. If not, then the narrow band data can be used to test the hypothesis that the spectra are rising rapidly (due to the Wien portion of a hot black body) or more slowly, along the extrapolation of power-law spectra from higher energies. The latter test is extremely important in the study of quasars (see above).

It is entirely possible that the ALEXIS and EUVE missions will be operating concurrently. The opportunity to quickly detect transients with ALEXIS and observe them in outburst with EUVE will allow studies of active regions on late type stars and hot spots in the disks of cataclysmic variables. Catching objects in outburst gives the best chance to measure the temperatures and abundances in these regions, because the regions are most easily isolated from other, more quiescent processes.

9.6 Synoptic Monitoring of Variable Sources

As ALEXIS continuously surveys a large fraction of the sky, it is of considerable interest to look at its potential for detecting transient sources of EUV/soft X-ray emission. Since there are no ALEXIS predecessors in

difficult to be rigorous in estimates of its capability for detecting transients, but the experience from X-ray surveys is encouraging. One pertinent study is that of Helfand and Vrulek (1983) who detected four very fast (1-10 s) flares in a survey of 3×10^6 s of Einstein IPC data (0.15 - 3.5 keV). From this data they deduced an all-sky event rate of $< 10^{-5}$ per year. Their limiting flux was 10 microJy. None of the Einstein transients have as of yet been identified. HEAO-1 X-ray data (0.5 - 20 keV) have also yielded a number of, as yet also unidentified, transients lasting 30 minutes or less (Connors, Serlemitsos and Swank 1986, Ambruster and Wood 1986). Pye and McHardy (1983) discovered longer time scale transients (few hours to 1 day) using the Ariel V Sky Survey instrument (2 - 18 keV). Some of these transients are known dMe flare stars or RS Canis Venaticorum (RS CVn) stars. Others, still unidentified, may also be of these classes of objects. A survey of 20 dwarf novae in outburst in the low-energy HEAO-1 data (0.15 - 0.5 keV) yielded two ultrasoft sources that were extremely bright for a few days (Córdova *et al.* 1980b). Other ultralow-energy X-ray sources discovered in surveys of unidentified soft HEAO-1 sources were the magnetic cataclysmic variable stars that can be in states of high mass accretion for months or years (see, e.g. Jensen, Nousek, and Nugen 1982). Some HEAO-1 ultrasoft transients still remain unidentified (e.g., Nousek, Córdova, and Garmire 1980). These X-ray surveys indicate that variability is common to stellar sources on all time scales, and in all the energy regions sampled thus far. Below we discuss the sensitivity of ALEXIS to such transient continuum and emission-line sources.

Accreting white dwarfs: ALEXIS will have a significant sensitivity to nearby hot white dwarfs and cataclysmic variables (mass-exchanging semi-detached binaries consisting of a white dwarf and a low-mass companion). Due to the high luminosities generated by the accretion of material onto white dwarfs ($L \sim 10^{35} M_{\odot} \text{ erg s}^{-1}$, where M_{\odot} is the accretion rate in units of 10^{-8} solar masses/yr), cataclysmic variables are intrinsically bright astronomical sources. Cataclysmic variables which accrete at high rates through an accretion disk (nova-like variables and dwarf novae in outburst) are bright EUV and soft X-ray sources: fully one-quarter of their accretion luminosity is emitted with a blackbody spectrum with a temperature of a few tens of eV (Córdova *et al.* 1980a, Patterson and Raymond 1985). Cataclysmic variables in which the dynamics of the accreting material is controlled by the magnetic field of the white dwarf (polars or AM Her stars) release about half of their accretion luminosity at EUV and soft X-ray energies and about half at temperatures of a few tens of keV. Because of their high space density and because they are intrinsically bright X-ray sources, cataclysmic variables make up a significant fraction of the number of sources found in any survey of the X-ray sky. Moreover, cataclysmic variables offer a unique laboratory for the study of the processes of mass accretion and mass loss manifest by such Galactic constituents as pre-main-sequence stars (e.g., T Tauri and FU Orionis stars), late-type stars, early-type stars (e.g., O-stars, giants, supergiants, and Wolf Rayet stars), symbiotic stars, low- and high-mass neutron star binaries, and accreting stellar-mass black holes (e.g., Cyg X-1 and SS 443). Furthermore, accretion onto--and mass ejection from--massive black holes are central to the dynamics of the our Galaxy and of active galactic nuclei and quasars. Because of these shared similarities, because of their variability and high space density and their intrinsically high UV, EUV, and X-ray luminosities, because they can routinely be observed from the ground with both large and small telescopes by both professional and amateur astronomers and (although infrequently) from space with ultraviolet, far ultraviolet, and X-ray satellites, cataclysmic variables offer a wealth of observational information on the processes of mass accretion and mass loss with which we have hope to better understand a large and diverse class of astrophysical objects.

Because cataclysmic variables radiate a significant fraction of their luminosity at EUV and soft X-ray energies, ALEXIS will have a significant sensitivity to this important class of objects. Assuming that the boundary layer between the accretion disk and the surface of the white dwarf in a non-magnetic cataclysmic variable radiates with a blackbody spectrum with a temperature of 25 eV and a luminosity of $4 \times 10^{34} \text{ erg s}^{-1}$, and discounting photoelectric absorption by intervening material, the source count rates in the 72, 82, and 107 eV bandpasses of the ALEXIS telescopes will be 3.7, 3.6, and $2.8 d_{100}^{-2} \text{ counts s}^{-1}$, respectively, where d_{100} is the distance to the cataclysmic variable in units of 100 pc. Since twice as much of the luminosity of magnetic cataclysmic variables is radiated at these temperatures compared to non-magnetic cataclysmic variables, the count rates for magnetic cataclysmic variables will typically be twice these values. Observations with soft X-ray experiments on HEAO-1, Einstein, and EXOSAT show that dwarf novae in outburst and magnetic variables have comparably strong fluxes in the 1/4 keV band. Since one optical depth at 72, 82, and 107 eV corresponds to $\sim 0.75, 1.15,$ and $2.05 \times 10^{19} \text{ atoms cm}^{-2}$ of intervening interstellar material, respectively, significant count rates in the various bandpasses can be realized for cataclysmic variables with distances of less than approximately 200 parsecs which have column densities of less than a few times $10^{19} \text{ atoms cm}^{-2}$. To illustrate that there are a number of cataclysmic variables which meet these criteria, consider the case of the four (non-magnetic) cataclysmic variables for which Marshall, Raymond, and Córdova (1988) have determined (by means of high resolution ultraviolet spectra) the column density of neutral interstellar material: IX Vel, SS Cyg, V3885 Sp, and RW Sex. The measured neutral hydrogen

column densities ($2.0\text{--}8.9 \times 10^{19} \text{ atoms cm}^{-2}$) and distances (95--150 pc) result (in three of the four cataclysmic variables) in significant count rates in the three ALEXIS bandpasses: the summed count rates for IX Vel, SS Cyg, and V3885 Sgr are determined to be 0.96, 0.75, and 0.13 counts s^{-1} , respectively, relative to a predicted background rate of ≤ 0.01 counts s^{-1} per resolution element. U Gem, VW Hyi, and approximately half a dozen other cataclysmic variables will likely be detected with comparable count rates, making the study of the soft X-ray luminosities of the boundary layers of cataclysmic variables a significant component of the science possible with ALEXIS.

Active, cool stars: The second group of candidates for soft X-ray transients are emission-line, rather than continuum, sources. These are the dMe flare stars and the RS CVn binaries. These objects were discovered as a large class of soft X-ray emitters by HEAO-1 and Einstein. Their X-ray emission arises in a hot, thin thermal plasma lying in the transition region and corona with a temperature between 10^5 and a few times 10^7 K (see Pye and McHardy 1987). Their variability is due to rotational modulation of active regions or flares. The latter can last from a few seconds up to a few hours (in some cases up to 10 days!), and may occur with a repetition cycle of a few days (Walter et al. 1987). In the binaries eclipses can also produce variability and are a useful diagnostic tool for determining the spatial distribution of coronal plasma (e.g., White et al. 1987).

The RS CVn sources were typically the same intensity in the Einstein IPC detector as were the dwarf novae U Gem and SS Cyg during outburst, that is, a few counts/sec. To estimate the sensitivity of ALEXIS to an emission-line source with the parameters of a RS CVn-like flare we folded the spectral parameters for HR 1099 (Walter 1988, private communication) through the response of the ALEXIS detecting system. For an emission integral of 10^{50} , a plasma temperature of 10^6 K, a radius of the emission region of 10 solar radii, and a distance to the source of 1 kpc (with no absorption), the estimated spectral line intensity of HR 1099 in the 72 eV band is $2.5 \text{ photons cm}^{-2} \text{ s}^{-1}$. This corresponds to a count rate of 1 count s^{-1} in one detector pixel, a factor of 100 above the most conservative estimate of the background count rate. For a temperature of 4×10^4 K, the source count rate is equal to the background rate. Therefore, bright RS CVn flares with temperatures of about one million degrees can be detected with ALEXIS in one pass over the source.

ALEXIS will be able to sample the orbital light curves of cool, active binaries. The typical orbital periods of RS CVn systems lie in the range 1 - 14 days. Any source will be in the ALEXIS field of view for six months at a time, with various duty cycles depending on the particular telescope that views the source and the ecliptic latitude of the source; the duty cycle is 32% in the best cases. Thus some RS CVn stars may be monitored by ALEXIS throughout a substantial fraction of a binary orbital period, for many binary orbits.

9.8 Search for Fast Transients

Perhaps the most exciting possible result from ALEXIS would be the discovery of fast transient phenomena in the ultrasoft X-ray region. ALEXIS will be monitoring more than 1 sr of sky at any instant, and is thus sensitive to transient phenomena on any timescale. The paired telescopes will give confirmation of any continuum transient event. Historically, instruments sensitive to transients in unexplored bands have led to discoveries. For example, Los Alamos detectors on the Vela satellites led to the discovery of gamma-ray bursts and the co-discovery of X-ray bursts. Perhaps similar luck will strike again.

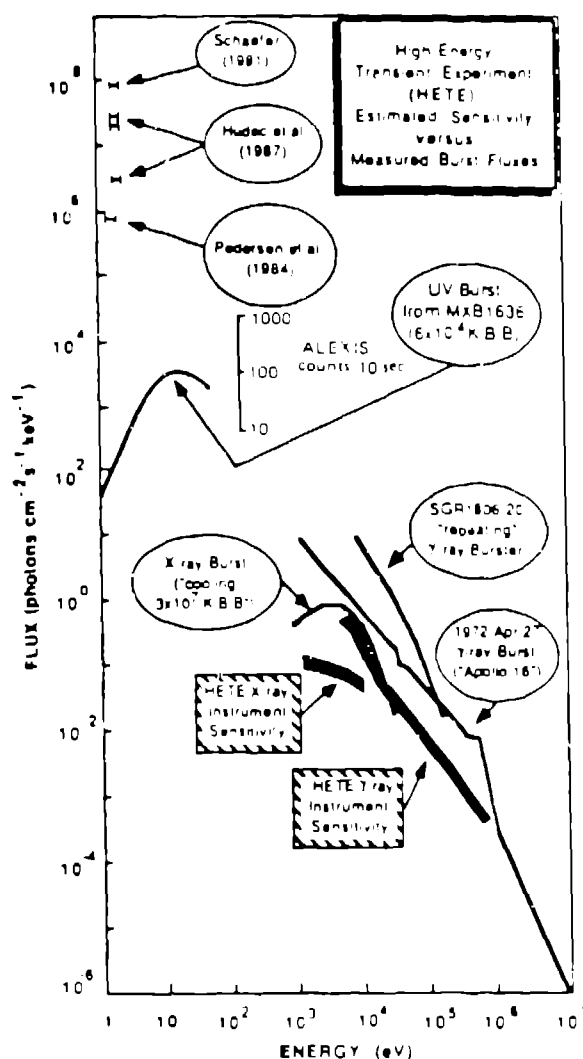


Figure 12: Broad-band signals from a gamma-ray burst, from Lamb (1988). Also shown are the expected count rates from ALEXIS for such an event

One possible fast transient is gamma-ray bursts, which may yield detectable signals in the ultrasoft X-ray band. Lamb (1988) summarizes data and theory on their broad-band spectra (Figure 12). Interpolating between measurements in the X-ray and optical bands, one might expect an ALEXIS signal of 50-500 counts in 10 seconds from a gamma-ray burst. If any ultrasoft X-ray signal is seen from a low-galactic latitude gamma burst, this will be proof that the bursts are nearby and not at cosmological distances. Sadly, so little is known about gamma bursts even 15 years after their discovery, that their distances are still unknown within a factor of 10^6 .

This work was performed under the auspices of the US Department of Energy. We would like to acknowledge comments on the manuscript by Drs. Diane Roussel Dupré and Chris Mauche.

REFERENCES

- Allen, C. W., "Astrophysical Quantities" (3rd edition), Athlone, London (1973).
- Ambruster, C.W., and Wood, K.S., *Ap.J.* 311, 258 (1986).
- Barbee, T. W. Jr., "Applications of thin film multilayer structures to figured X-ray optics", *Proc. SPIE* 563, 2-28 (1985).
- Barbee, T. W. Jr., Mrowka, S., and Hettrick, M. C., "Molybdenum-silicon multilayer mirrors for the extreme ultraviolet", *Appl. Optics* 24, 883-886 (1985).
- Bechtold, J., Czerny, B., Elvis, M., Fabbiano, G., and Green, R.F., "X-ray Spectra of PG Quasars II. The X-ray-Ultraviolet Excess of PG 1211+143", *Ap. J.* 314, 699 (1986).
- Bisnovatyi-Kogan, G.S., and Blinnikov, S. I. "Disk accretion onto a Black Hole at Subcritical Luminosity," *Astron. and Astrophys.* 59, 111 (1977).
- Bloch, J. J., "Observations of the diffuse soft X-ray background from 0.07 to 1.0 keV", Ph. D. thesis, University of Wisconsin-Madison (1988).
- Bloch, J. J., Jahoda, K., Juda, M., McCammon, D., Sanders, W. T., and Snowden, S. L., "Observations of the soft X-ray diffuse background at 0.1 keV", *Ap. J. (Letters)* 308, L59-62 (1986).
- Connors, A., Serlinitos, P.J. and Swank, J.H., "Fast Transients: a Search in X-Rays for Short Flares, Bursts, and Related Phenomena", *Ap. J.* 303, 769 (1986).
- Córdova, F., Chester, T. J., Tuohy, I. R., and Garmire, G. P., *Ap. J.* 235, 163 (1980a).
- Córdova, F., Nugent, J.J., Klein, S.R., and Garmire, G.P., *MNRAS* 190, 87 (1980b).
- Deharveng, J. M., Riviere, G. P., Monnet, G., Moutonnet, J., Courtes, G., Deshayes, J. P., and Berges, J. C., "FAUST Instrument: A high focal ratio telescope for far and near UV imagery", *Space Sci. Instrum.* 5, 21-35 (1979).
- Fleeter, R., "Miniature satellite technology applications", *Proceedings SPIE* 982, 173-187 (1988).
- Fraser, G. W., Pearson, J. G., Smith, G. C., Lewis, M., and Barstow, M. A., "The gain characteristics of microchannel plates for X-ray photon counting", *IEEE Trans. Nucl. Sci.* NS-30, 455-460 (1983).
- Fritz, T. A., *et al.*, "Significant initial results from the environmental measurements experiment on ATS 6", *NASA T. P.* 1101 (1977).
- Galeev, A. A., Rosner, R. and Vaiana, G. S. 1979, "Structured Coronae of Accretion Disks," *Ap. J.* 229, 318 (1979).
- Giommi, P., Tagliaferri, G., and Angelini, L., "Serendipitous sources in EXOSAT images", to appear in "Space Astronomy with EXOSAT", ed. N. E. White and R. Pallavicini (1988).
- Golub, L., Hamden, F. R., Jr., Maxson, C. W., Rosner, R., Vaiana, G. S., Cash, W., and Snow, T. P., "EINSTEIN observations of X ray emission from A stars", *Ap. J.* 271, 264-270 (1983).
- Haisch, B. M. *et al.*, "Simultaneous X ray, ultraviolet, optical, and radio observations of the flare star Proxima Centauri", *Ap. J.* 245, 1009-1017 (1981).
- Harwit, M., "Cosmic Discovery", Basic Books, New York, 1981.

Heise, J., Brinkman, A. C., Schrijver, J., Mewe, R., Gronenschild, E., den Boggende, A., and Grindlay, J., "Evidence for X-ray emission for flare stars observed by ANS", *Ap. J. (Letters)* 202, L73-76 (1975).

Helfand, D.J., and Vrtillek, S.D., *Nature* 304, 41 (1983).

Inoue, H., Koyama, K., Matsuoka, M., Ohashi, T., Tanaka, Y., and Tsunemi, H., "Evidence of OVII Emission Line in Diffuse Soft X-Rays from the NH Minimum Region in Hercules", *Ap. J. (Letters)* 227, L85 (1979).

Jensen, K., Nousek, J., and Nugent, J., *Ap. J.* 261, 625 (1982).

Kahn, S. M., Linsky, J. L., Mason, K. O., Haisch, B. M., Bowyer, C. S., White, N. E., and Pravdo, S. H., "HEAO-1 Observations of X-ray emission from flare stars observed by ANS", *Ap. J. (Letters)* 234, L107-L111 (1979).

Lamb, D. Q., "Theories of gamma-ray burst spectra", to appear in *Nuclear Spectroscopy of Astrophysical Sources*, AIP Conference Proceedings of the Workshop held 13-16 December 1987 in Washington, D. C., ed. N. Gehrels and G. Share.

Lockman, F.J., Jahoda, K., and McCammon, D. "The Structure of Galactic H I in Directions of Low Total Column Density," *Ap. J.* 302, 432-449 (1986).

Long, K. S., and White, R. L., "A survey of soft X-ray emission from hot stars", *Ap. J. (Letters)* 239, L65-68 (1980).

Maggio, A., Sciortino, S., Vaiana, G. S., Majer, P., Bookbinder, J., Golub, L., Harnden, F. R., Jr., and Rosner, R., "Einstein observatory survey of X-ray emission from solar-type stars: the late F and G dwarf stars", *Ap. J.* 315, 687-699 (1987).

Malina, R. F., Bowyer, S., Lampton, M., Finley, D., Paresce, F., Penegor, G., and Heetericks, H., "The Extreme Ultraviolet Explorer", *Optical Engineering* 21, 764-768 (1982).

Mauche, C.W., Raymond, J.C., and Córdova, F.A., *ApJ*, in press (1988).

McCammon, D., Burrows, D. N., Sanders, W. T., and Kraushaar, W. L., *Ap. J.* 269, 107 (1983).

Nousek, J., Córdova, F., and Garmire, F., *ApJ*. 242, 1107 (1986).

Palik, E. B., "Handbook of Optical Constants of Solids", Academic Press (1985).

Parker, R. A. R., Gull, T. R., and Kirshner, R. P., "An Emission Line Survey of the Milky Way", *NASA SP-433* (1979).

Patterson, J., and Raymond, J. C., *Ap. J.* 292, 550 (1985).

Friedhorsky, W. C., Bloch, J. J., Smith, B. W., Strobel, K., Ulibarri, M., Chavez, J., Evans, E., Siegmund, O. H. W., Marshall, H., Vallerga, J., and Vedder, P., "ALEXIS: An Ultraviolet X-Ray Monitor Experiment Using Miniature Satellite Technology", *Proceedings SPIE* 982, 188-207 (1988).

Pounds, K., "The EXOSAT X-ray spectral survey of emission line galaxies", in *IAU Symposium 134, "Active Galactic Nuclei"*, in press (1988).

Pounds, K., Stranger, V.J., Turner, T.J., King, A.R., and Czerny, B., "Discovery of Strong Soft X-ray Excess in Mk 335 - Evidence for an Accretion Disk?", *M.N.R.A.S.* 224, 443, (1987).

Pye, J.P., and McHardy, I.M., *MNRAS* 205,875 (1983).

Pye, J.P., and McHardy, I.M., *Proc. of the Conf. on "Activity in Cool Star Envelopes"*, Tromsø, Norway, July (1983).

- Raymond, J. C., and Smith, B. W. 1977, "Soft X-Ray Spectrum of a Hot Plasma", *Ap. J. (Suppl.)* 35, 419 (1977).
- Rosner, R., *et al.*, "The stellar contribution to the Galactic soft X-ray background", *Ap. J. (Letters)* 249, L5-9 (1981).
- Schmitt, J. H. M. M., Golub, L., Hamden, F. R., Jr., Maxson, C. W., Rosner, R., and Vaiana, G. S., "An Einstein observatory X-ray survey of main-sequence stars with shallow convection zones", *Ap. J.* 290, 307-320 (1985).
- Shakura, N.I., and Sunyaev, R.A., "Black Holes in Binary System: Observational Appearance," *Astron. and Astrophys.* 24, 337 (1973).
- Shemansky, D.E., "Ratio of Oxygen to Sulfur in the Io Plasma Torus," *J. Geophys. Res.* 92, 6141-6146 (1987).
- Siegmund, O. H. W., Lampton, M., Bikler, J., Chakrabarti, S., Vallergha, J., Bowyer, S., and Malina, R., "Wedge and strip image readout systems for photon-counting detectors in space astronomy", *J. Opt. Soc. Am.* 3, 2139-2148 (1986).
- Siegmund, O. H. W., Lampton, M., Bikler, J., Vallergha, J., and Bowyer, S., "High efficiency photon counting detectors for the FAUST Spacelab far ultraviolet observatory payload", *IEEE NS-34*, 41 (1987).
- Siegmund, O. H. W., Vallergha, J., and Lampton, M., "Background events in microchannel plates", *IEEE Trans. Nucl. Sci.* NS-35, 524-528, Feb. (1988).
- Siegmund, O. H. W., "Investigations of bonded and curved microchannel plate stacks", *Proceedings SPIE* 982, 108-114 (1988).
- Trümper, J., "ROSAT", *Physica Scripta* T7, 209-215 (1984).
- Vallergha, J., Siegmund, O. H. W., Everman, E., and Jelinsky, P., "Calibration of thin film filters to be used on the Extreme Ultraviolet Explorer satellite", *Proceedings SPIE* 689, 138-143 (1986).
- Walker, A. B. C., Jr., Barbee, T. W., Jr., Hoover, R. B., and Lindblom, J. F., "Soft X-Ray Images of the Solar Corona with a Normal Incidence Cassegrain Multilayer Telescope", *Science* 241, 1781-1787 (1988).
- Walter, F., *et al.*, *Astron. Ap.* 186, 241 (1987).
- Wilkes, B. J., and Elvis, M., "Soft X-Ray spectra of quasars", *Ap. J.* 323, 243-262 (1987).
- Windt, D. L., "The optical properties of 21 thin film materials in the 10 eV to 500 eV photon energy region", Ph.D. thesis, University of Colorado-Boulder (1987).
- White, N., *et al.*, in *Proc. of 5th Cambridge Workshop on "Cool Stars, Stellar Systems, and the Sun"*, in press (1987).

